J. Dairy Sci. 107:2026–2046
https://doi.org/10.3168/jds.2023-23447

Valine and nonessential amino acids affect bidirectional transport rates of leucine and isoleucine in bovine mammary epithelial cells

A. Hruby Weston,[1]* I. A. M. A. Teixeira,[1,2] P. S. Yoder,[1,3] T. Pilonero,[1] and M. D. Hanigan[1]
[1]School of Animal Sciences, Virginia Tech, Blacksburg, VA 24060
[2]Department of Animal, Veterinary, and Food Sciences, University of Idaho, Twin Falls, ID 83303-1827
[3]Perdue AgriBusiness LLC, Salisbury, MD 21804

ABSTRACT

A more complete understanding of the mechanisms controlling AA transport in mammary glands of dairy cattle will help identify solutions to increase nitrogen feeding efficiency on farms. It was hypothesized that Ala, Gln, and Gly (NEAAG), which are actively transported into cells and exchanged for all branched-chain AA (BCAA), may stimulate transport of BCAA, and that Val may antagonize transport of the other BCAA due to transporter competition. Thus, we evaluated the effects of varying concentrations of NEAAG and Val on transport and metabolism of the BCAA Ala, Met, Phe, and Thr by bovine mammary epithelial cells. Primary cultures of bovine mammary epithelial cells were assigned to treatments of low (70% of mean in vivo plasma concentrations of lactating dairy cows) and high (200%) concentrations of Val and NEAAG (LVal and LNEAAG, HVal and HNEAAG, respectively) in a 2 × 2 factorial design. Cells were preloaded with treatment media containing [^{15}N]-labeled AA for 24 h. The [^{15}N]-labeled media were replaced with treatment media containing [^{13}C]-labeled AA. Media and cells were harvested from plates at 0, 0.5, 1, 5, 15, 30, 60, and 240 min after application of the [^{13}C]-labeled AA and assessed for [^{15}N]- and [^{13}C]-AA label concentrations. The data were used to derive transport, transamination, irreversible loss, and protein-synthesis fluxes. All Val fluxes, except synthesis of rapidly exchanging tissue protein, increased with the HVal treatment. Interestingly, the rapidly exchanging tissue protein, transamination, and irreversible-loss rate constants decreased with HVal, indicating that the significant flux increases were primarily driven by mass action with the cells resisting the flux increases by downregulating activity. However, the decreases could also reflect saturation of processes that would drive down the mass-action rate constants. This is supported by decreases in the same rate constants for Ile and Leu with HVal. This could be due to either competition for shared transamination and oxidation reactions or a reduction in enzymatic activity. Also, NEAAG did not affect Val fluxes, but influx and efflux rate constants increased for both Val and Leu with HNEAAG, indicating an activating substrate effect. Overall, AA transport rates generally responded concordantly with extracellular concentrations, indicating the transporters are not substrate-saturated within the in vivo range. However, BCAA transamination and oxidation enzymes may be approaching saturation within in vivo ranges. In addition, System L transport activity appeared to be stimulated by as much as 75% with high intracellular concentrations of Ala, Gln, and Gly. High concentrations of Val antagonized transport activity of Ile and Leu by 68% and 15%, respectively, indicating competitive inhibition, but this was only observable at HNEAAG concentrations. The exchange transporters of System L transport 8 of the essential AA that make up approximately 40% of milk protein, so better understanding this transporter is an important step for increased efficiency.

Key words: amino acid transport, mathematical model, stable isotope, mammary gland, bovine

INTRODUCTION

Excess nitrogen in dairy cattle diets is excreted in waste, which contributes to increased ammonia emissions from dairy farms. Increasing N efficiency in milk production is key to decreasing N excretion, and efficiency improvement requires an in-depth understanding of AA metabolism. Before 2021, requirements for AA were generally calculated in aggregate as MP (NRC, 2001). The inability to balance for individual AA generally results in overfeeding of AA and MP, resulting in increased N excretion or in less-than-desired milk protein production. Abundant research supports the effects of Lys (Schwab et al., 1976), Met (Rulquin and Delaby, 1997), although inconsistent (Patton, 2010), and His

Received March 2, 2023.
Accepted September 27, 2023.
*Corresponding author: achruby@vt.edu

(Vanhatalo et al., 1999; Lee et al., 2012) on milk-protein production. Recently, NASEM (2021) quantified milk protein responses to His, Ile, Leu, Lys, and Met, in addition to an aggregated term consisting of the remaining EAA plus NEAA. Certainly, advancements have been made, but there is evidence of responses to individual AA within the aggregated AA and potential interactions among AA that have not been fully evaluated. To investigate these interactions, we need to examine the mechanisms underpinning potential interactions, which includes the AA transporters.

Amino acid transporters within bovine mammary epithelial cells (**MEC**) are affected by a plethora of influences, including the extracellular and intracellular concentrations of the AA they transport (Baumrucker, 1984; Christensen, 1990; Maas et al., 1998; Hanigan et al., 2000; Wu, 2013; Shennan and Boyd, 2014; Taylor, 2014; Bröer and Bröer, 2017). Most of the transporters are promiscuous in that they transport multiple AA, although generally a varying affinity exists for each AA. Transport mechanisms include passive diffusion, Na-dependent transport, and exchange transport. The combination of varying transport mechanisms and promiscuity yields mixed kinetics, often with a saturable, high-affinity component representing active transport and a lower affinity, nonsaturable component representing passive diffusion (Shotwell et al., 1981; Christensen, 1990). The saturable component is further complicated by varying affinities for the same AA across transporters (Bröer, 2008) and the use of some AA in exchange, also known as bidirectional reactions (Oxender and Christensen, 1963). Of particular interest is the System L bidirectional transporter, which is responsible for transporting 8 of the EAA that make up approximately 40% of milk protein. The bidirectional transporters operate with 1:1 stoichiometry, exchanging one intracellular AA for an extracellular AA and the reverse. Intracellular AA that are present in high concentrations, which includes those transported by unidirectional, energy-consuming transporters such as System A (Verrey, 2003), help drive net transport into the cell and maintain high intracellular concentrations.

Valine is a branched-chain AA (**BCAA**) transported by the transporters of System L. Deletion of Val tended to decrease milk-protein production and decreased milk-protein concentrations in dairy cows; however, Leu was also unintentionally low, which prevented previous authors from ruling out its role in this effect (Haque et al., 2013). Prior research also discussed the possibility that this effect was caused by interactions or antagonisms among the BCAA. Interestingly, NASEM (2021) observed that Val was negatively related to milk-protein production in half of 5,000 generated models evaluated, indicating a possible AA antagonism as the Val supply increased. Furthermore, an abomasal infusion of EAA without Leu increased plasma Val and Ile by 60% and 70%, respectively, compared with an abomasal infusion of all EAA in lactating dairy cows (Doelman et al., 2015). Possible competition at high concentrations is further supported by increased and decreased concentrations of Ile and Val in plasma with a diet deficient in Leu (Tian et al., 2017) and high dietary Leu concentrations (Rulquin and Pisulewski, 2006), respectively, in dairy cattle. However, the mechanism of such an interaction has not been delineated in dairy animals.

Alanine, Gln, and Gly are actively transported by the Na-dependent System A transporter and used as exchange currencies by System L and other bidirectional transporters. Seymour et al. (1990) concluded that demand for NEAA increased with combined infusions of Met and Lys in lactating dairy cows based on observations of increased Gln concentrations. Both Ala and Gln are released during catabolism of BCAA (Holeček, 2018). Furthermore, Ala and Gln are both N donors involved with reamination of BCAA (Sperringer et al., 2017). These NEAA may also influence uptake of EAA via the bidirectional transporters.

Most prior AA transport measurements in mammary tissue or cells have considered only net flux (Jackson et al., 2000; Li et al., 2009). However, net flux information is of limited value, particularly for transporters using exchange mechanisms. Hanigan et al. (2009) described an in vivo method of assessing bidirectional mammary transport and metabolism for Phe, and Yoder et al. (2020a) adapted and extended the method for use with additional AA in cultured cells. Using this method, total transport activity for each AA can be directly assessed in the native cellular state rather than inferred from non-metabolizable analogs, thereby allowing assessment of the overall kinetic response and interactions among AA.

Thus, the objective of this study was to use the method developed by Yoder et al. (2020a) to evaluate 2 possible drivers of AA transport in MEC: substrate competition and exchange currency influence. We used Val individually and Ala, Gln, and Gly as a group (**NEAAG**) to assess those mechanisms. We hypothesized that (1) high concentrations of Val would competitively inhibit uptake of other AA by System L, especially other BCAA, and (2) increased concentrations of NEAAG would increase uptake of AA catalyzed by System L exchange transporters.

MATERIALS AND METHODS

Because no human or animal subjects were used, this analysis did not require approval by an Institutional Animal Care and Use Committee or Institutional Review Board.

Experimental Design, Materials, and Protocol

Primary bovine MEC of unknown passage number derived from a lactating cow were obtained from the State Key Laboratory of Animal Nutrition, Institute of Animal Science, Chinese Academy of Agricultural Sciences, Beijing, China, and transferred to Virginia Tech, Blacksburg, Virginia. Cells were prepared as described by Hu et al. (2009) and stored frozen in liquid nitrogen. Upon arrival, cells were confirmed to be of bovine epithelial origin (Yoder et al., 2019) and to produce casein (Ruiz-Cortés et al., 2022). Cells were then routinely passaged 6 times before use in this experiment.

Treatments were arranged in a 2 × 2 factorial design with factors of low and high Val concentration (**LVal** and **HVal**), and low and high NEAAG concentrations (**LNEAAG** and **HNEAAG**). The low and high concentrations were 70% and 200% of in vivo plasma concentrations (Yoder et al., 2020b), respectively, which approximately reflects the normal in vivo plasma concentration range in dairy cows (Martineau et al., 2017).

Cells were thawed and seeded into tissue-culture-treated T-75 flasks (no. 353135, Corning Inc., Corning, NY) at approximately 2.1×10^6 density and incubated at 37°C under 5% CO_2 (HERAcell 150i, Thermo Fisher Scientific, Waltham, MA). Cell growth media consisted of Dulbecco's Modified Eagle Medium/Nutrient Mixture F-12 (no. 12400024, Gibco, Waltham, MA) containing sodium bicarbonate (1.2 g/L), 10% fetal bovine serum (no. F2442, Sigma-Aldrich, St. Louis, MO), and 1% of a 100× antibiotic–antimycotic mix (no. 15240062, Gibco, Waltham, MA). All media were sterile filtered before use (no. 595-4329, Thermo Fisher Scientific, Waltham, MA). Cells were expanded in growth media, pooled at the final passage, and used to seed 96 preweighed 100-mm tissue-culture-treated plates (no. 353003, Corning Inc., Corning, NY) with approximately 3.9×10^4 cells/cm^2. The seeded cells were incubated in growth medium until they reached >90% confluency, which took approximately 48 h.

For the experiment, cells were incubated for a total of 24 h in 2 changes of acclimation medium; the intent was to minimize AA concentration changes over time. The fetal bovine serum–free acclimation medium consisted of an AA- and fatty acid-free, custom Dulbecco's Modified Eagle Medium/Nutrient Mixture F-12 (Thermo Fisher Scientific, Waltham, MA) supplemented with individual AA to achieve a concentration profile similar to that of lactating dairy cow plasma (Yoder et al., 2020b; Supplemental Table S1; https://doi.org/10.7294/24042825, Hruby et al., 2023). Acclimation and treatment media contained 1.2 g/L of sodium bicarbonate, 1% of antibiotic–antimycotic mix, 5 mg/L of bovine insulin (no. I6634, Sigma-Aldrich, St. Louis, MO), 5 mg/L of bovine prolactin (no. AFP7170E, A. F. Parlow, National Hormone and Pituitary Program, National Institute of Diabetes and Digestive and Kidney Diseases, National Institutes of Health, Torrance, CA), 5 mg/L of transferrin (no. T8158, Sigma-Aldrich, St. Louis, MO), 1 mg/L of hydrocortisone (no. H0888, Sigma-Aldrich, St. Louis, MO), 0.01 mg/L of epidermal growth factor (no. E4127, Sigma-Aldrich, St. Louis, MO), and 5 mg/L of progesterone (no. P7556, Sigma-Aldrich, St. Louis, MO). The hormone profile replicated that described by Yoder et al. (2020a). At the end of the acclimation period, all plates were washed 3 times with warm PBS, and the acclimation medium was replaced with 1 of 4 randomly assigned treatment media containing universally labeled [^{15}N]-AA derived from algae (no. NLM-2161, Cambridge Isotope Laboratories Inc., Tewksbury, MA; [^{15}N]-labeled treatment media; Table 1). Before treatment application, plates were labeled with a unique identification and then were randomly matched to treatments. [^{15}N]-labeled treatment media were changed every 8 h to minimize depletion of AA. After 24 h, [^{15}N]-labeled treatment media were removed, cells were washed 3 times with warm PBS, and 6 mL of treatment medium containing universally labeled [^{13}C]-AA derived from algae (no. CLM-1548, Cambridge Isotope Laboratories Inc., Tewksbury, MA) was added. All treatment media contained AA in the same concentrations as the acclimation medium, except for the 4 AA being manipulated as treatments (Val and NEAAG). Labeled AA concentrations were held constant across treatments, and the unlabeled AA were manipulated to achieve the desired treatment concentrations.

Plates were randomly assigned within treatment-to-collection time points (0, 0.5, 1, 5, 15, 30, 60, and 240 min), and harvested as specified with the exact harvest time recorded for each. At harvest, 1 mL of medium was sampled and stored at −20°C, and the remaining medium was discarded. Cells were washed 3 times with cold PBS and the plates were weighed. Cells were lysed by the addition of 1 mL (preweighed) of 50% sulfosalicylic acid and mechanically scraped (scraper no. 353085, Corning Inc., Corning, NY). The scraped lysate was collected and stored at −20°C until analysis.

Amino Acid Measurements

Media samples collected during the experiment were gravimetrically weighed, and 50% sulfosalicylic acid was added to achieve a final concentration of 8%. Acidified media and cell homogenates were centrifuged at 16,000 × *g* for 15 min at 4°C. Media and cell supernates were

Table 1. Mean unlabeled AA concentrations (Conc; μ*M*), SD,[1] and isotope ratios (IR)[2] by treatment[3] in the [^{15}N]-labeled extracellular media before cell exposure

	Treatment											
	LNEAAG, LVal			LNEAAG, HVal			HNEAAG, LVal			HNEAAG, HVal		
AA	Conc	SD	IR	Conc	SD	IR	Conc	SD	IR	Conc	SD	IR
Ala	75.2	6.22	2.36	78.9	10.8	2.44	456	22.1	0.52	458	28.2	0.52
Arg	44.5	2.92	—	47.8	6.07	—	45.1	1.10	—	47.4	4.23	—
Asp	11.0	0.90	9.69	12.1	1.24	9.58	11.5	0.32	9.54	12.5	1.73	9.38
Gln	37.3	9.75	—	37.1	7.48	—	86.5	4.08	—	83.1	4.36	—
Glu	82.0	7.26	2.15	64.0	8.92	2.81	120	6.03	1.62	118	4.29	1.64
Gly	158	10.6	—	167	21.4	—	603	19.1	—	597	37.2	—
His	71.4	7.33	—	82.0	11.9	—	72.8	4.36	—	78.7	10.0	—
Ile	60.9	5.89	1.33	67.0	10.6	1.34	62.9	3.56	1.33	66.7	7.82	1.34
Leu	114	2.88	1.30	119	17.9	1.30	112	5.96	1.31	119	13.3	1.29
Lys	26.3	1.52	2.67	27.1	1.95	2.63	26.7	1.53	2.79	28.9	4.16	2.75
Met	5.21	0.03	4.92	5.26	0.48	5.17	5.06	0.13	5.15	5.24	0.32	4.98
Phe	8.63	0.23	10.2	9.16	0.48	10.5	8.88	0.40	10.2	9.09	0.40	10.4
Pro	62.4	6.29	1.00	68.0	10.8	1.00	64.3	3.28	1.00	68.5	8.31	1.00
Ser	63.8	5.28	0.79	69.3	9.40	0.80	65.5	2.86	0.80	69.3	7.09	0.80
Thr	61.9	5.41	1.18	67.8	9.65	1.17	63.7	2.64	1.18	67.4	6.58	1.18
Tyr	2.19	0.22	10.6	2.23	0.53	11.3	2.10	0.20	11.3	2.25	0.31	11.4
Val	130	12.2	0.96	567	79.9	0.38	136	4.59	0.95	565	69.3	0.37

[1]Representative of 3 samples.

[2]IR = $\frac{^{15}N}{^{12}C}$.

[3]LNEAAG = low nonessential AA group (70% of in vivo concentrations of Ala, Gln, and Gly); HNEAAG = high nonessential AA group (200% of in vivo concentrations of Ala, Gln, and Gly); LVal = low Val (70% of in vivo concentration); HVal = high Val (200% of in vivo concentration).

collected and stored at −20°C. Cell pellets were rinsed twice with 500 μL of PBS and centrifuged for 6 min at 16,000 × *g* at 4°C, the supernates were discarded, and the pellets were stored at −20°C.

Media and cell supernates were subsequently thawed on ice and vortexed, a subsample was taken and weighed, and 250 μL of 2 external tracers were gravimetrically added. The first tracer solution contained 0.3 g/L of U-[^{13}C-^{15}N]-AA derived from algae (no. CNLM-452, Cambridge Isotope Laboratories Inc., Tewksbury, MA), 0.1 m*M* [$^{2}H_5$]-L-tryptophan (no. DLM-1092, Cambridge Isotope Laboratories Inc., Tewksbury, MA), and 0.35 m*M* [$^{13}C_2$]-labeled L-histidine (no. CLM-1512, Cambridge Isotope Laboratories Inc., Tewksbury, MA) dissolved in 0.1 *N* HCl. The second tracer solution contained 0.15 m*M* [^{13}C–^{15}N]-labeled L-glutamine (no. CNLM-1275, Cambridge Isotope Laboratories Inc., Tewksbury, MA) dissolved in double-distilled H_2O. The same external tracers were also added to the cell pellets, and the protein-bound AA were released by acid hydrolysis in 6 *N* HCl with 0.1% phenol, layered with N_2 gas, at 150°C for 70 min and filtered as described by Walsh et al. (2014).

Acid hydrolysates, media, and cell supernate samples were desalted and derivatized according to Calder et al. (1999). The AA derivatives were separated by GC (Thermo Trace 1310 GC equipped with a TriPlus RSH autosampler; Thermo Fisher Scientific, Waltham, MA) and quantified using a single-quadrupole MS operated in selected-ion-monitoring mode (ISQ LT system, Thermo Fisher Scientific, Waltham, MA). Ion masses that were monitored for each AA are described in Supplemental Table S2 (https://doi.org/10.7294/24042825, Hruby et al., 2023). Elution times were adjusted every 2 wk based on elution times of an AA standard (no. 20088, Thermo Fisher Scientific, Waltham, MA) with Gln, Asn, Trp, and Cys added. Concentrations were calculated from isotope ratios (**IR**) using SAS software (SAS Institute Inc., Cary, NC) and a gravimetrically prepared calibration curve consisting of increasing masses of unlabeled AA and constant masses of external tracer.

Model Calculations and Adjustments

All of the remaining data handling, statistics, and modeling work was completed by using R (v. 4.2.1) in RStudio (R Core Team, 2022). The differential equations for the dynamic system of equations used to derive flux values from the IR data were as described by Yoder et al. (2020a) with minor modifications to better reflect metabolism. For reference, a schematic of the unlabeled pools and fluxes is provided in Figure 1. These were mirrored by pools for the [^{13}C]- and [^{15}N]-labeled pools. Herein, fluxes or pools of [^{13}C] and [^{15}N] will be denoted by *i* and *ii*, respectively.

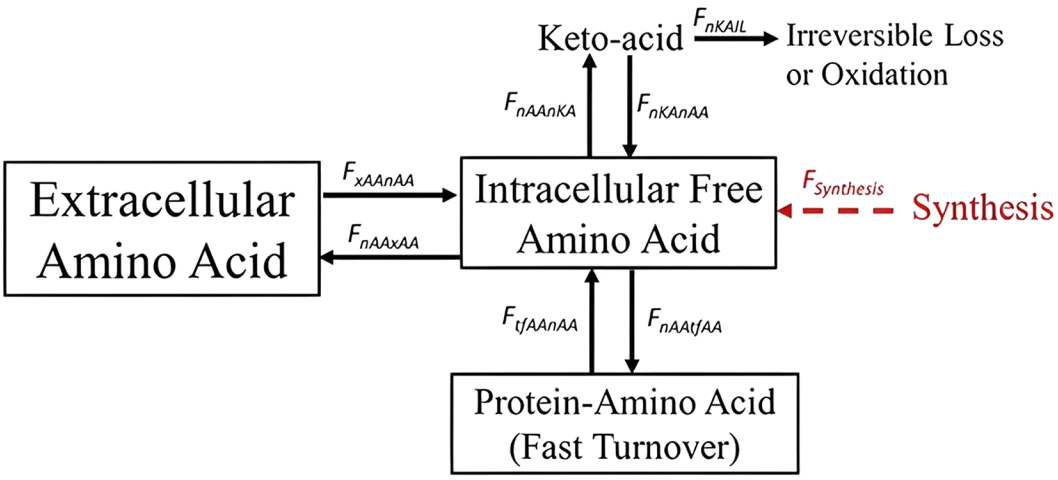

Figure 1. Unlabeled model schematic with boxes representing pools and arrows representing fluxes. The schematics for [^{15}N] and [^{13}C] are mirrored to the unlabeled fluxes and pools. The pools are extracellular amino acid (Q_{xAA}), intracellular free amino acid (Q_{nAA}), and protein-amino acid (fast protein synthesis; Q_{pAA}). The flux abbreviations are as follows: F_{xAAnAA} is the flux from extracellular AA to intracellular free AA, F_{nAAxAA} is the flux from intracellular free AA to extracellular AA, F_{nAAnKA} is the flux from intracellular free AA to keto acid, F_{nKAnAA} is the flux from keto acid returning to the intracellular free AA pool, F_{nAAIL} is the flux from keto acid to irreversible loss, $F_{nAAtfAA}$ is the flux of intracellular free AA to fast protein synthesis AA, $F_{tfAAnAA}$ is the flux of fast protein synthesis AA back to intracellular free AA, $F_{synthesis}$ is the flux of de novo amino acids into the intracellular free AA pool (this flux is in red to indicate that it only applies to the nonessential amino acids).

Initial pool sizes were calculated as measured concentrations multiplied by volume, where the extracellular volume ($\mathbf{V_x}$) was 6 mL; the intracellular bound protein volume ($\mathbf{V_p}$) was calculated as 17.5% of the difference between the washed-plate mass and the empty-plate mass after cell lysis and scraping at the end of the experiment (Yoder et al., 2021); and the intracellular free volume ($\mathbf{V_n}$) was calculated as 82.5% of the mass difference. The empty and full collection tubes were weighed, along with the V_n alone, but the aforementioned calculations were determined to be more accurate due to propagation of measurement errors when determining from 3 mass measurements. It is important to note that cell pellets were not dried, so the intracellular bound data herein represented wet cell pellets. Initial sizes for the fast-protein-synthesis and slow-protein-synthesis pools were calculated according to Yoder et al. (2020a), and the fast-protein-synthesis fraction was set at 6% for all AA according to in vivo data (Hanigan et al., 2006). Even with an additional time point versus that of Yoder et al. (2021), we were unable to identify unique rate constants for both slow protein synthesis and fast protein synthesis. Thus, the mass-action rate constant for slow protein synthesis ($k_{nAAtsAA}$) was set to 11.1% of the rate constant for fast protein synthesis, which reflects the ratio of the 2 rate constants derived by Hanigan et al. (2009).

In the past, we isolated casein proteins by acidification at pH 4.6; however, approximately 51% of the precipitated proteins are not caseins (Appuhamy et al., 2014). Given that level of contamination, we chose not to attempt to separate cell and milk proteins, which resulted in a fast-protein-synthesis pool that represented constitutive cell protein plus export proteins remaining in the cell.

Flux equations were all mass action as described by Yoder et al. (2020a). An example flux equation is provided for reference in Equation [1]:

$$F_{xAAnAA} = k_{xAAnAA} \times Q_{xAA}, \quad [1]$$

where F_{xAAnAA} is the flux of extracellular AA (x) to intracellular free AA (n; μmol/min), k_{xAAnAA} is the mass-action rate constant for the x to n movement (per minute), Q_{xAA} is the unlabeled pool size of AAx (μmol). The flux of AAn to the fast protein synthesis pool ($F_{nAAtfAA}$) was calculated in the same manner, except the precursor pool was intracellular free AA (Q_{nAA}). As previously described, tissue fast protein degradation ($F_{tfAAnAA}$) was set equal to $F_{nAAtfAA}$, reflecting steady-state cell protein mass. Although this is not completely representative of the biology, due to the approximate 1 to 2% of casein that would make up the cell protein, we concluded that the consideration of this would make little change to the final parameters.

Modifications relative to Yoder et al. (2021) were as follows. Due to high correlation between transamination and oxidation, the fixed kinetic rate constants for oxidation were converted to a fractional proportion of the transamination flux. This is biologically justified because AA are generally transaminated or deaminated before oxidation (Harris et al., 2005), and therefore the

latter must depend on the former. Thus, the equation for the flux of keto acid to irreversible loss of AA was

$$F_{nAAIL} = F_{nAAnKA} \times f_{nkAAIL}, \quad [2]$$

where F_{nAAIL} is the flux of n to irreversible loss (IL; μmol/min), F_{nAAnKA} is the flux of n to transaminated products (KA, generally keto acids; μmol/min), and f_{nkAAIL} is the fractional proportion of KA that are IL.

The majority of AA undergo transamination; if AA are reaminated it is possible that some [^{15}N]-label will be reincorporated into the [^{15}N] label–free AA pools. This was calculated as a function of the mean IR of Asp, Ala, and Gln over time to reflect the primary pools of N used for transamination (Krishnamurthy et al., 2017; Sperringer et al., 2017). The mean IR were predicted at any time from an exponential decay equation fitted to the [^{15}N] IR by treatment:

$$IR_{nKAii} = y_{KAii} \times e^{-k_{KAii} \times t} + a_{KAii}, \quad [3]$$

where IR_{nKAii} was the reamination IR factor at any point in time (t), and y_{KAii}, k_{KAii}, and a_{KAii} were fitted constants. An example of the observed IR and the derived prediction line is displayed in Supplemental Figure S1 (https://doi.org/10.7294/24042825, Hruby et al., 2023). Given these predictions, $F_{nKAnAAii}$ was calculated as

$$F_{nKAnAAii} = F_{nAAnKA} \times IR_{nKAii}. \quad [4]$$

Methionine metabolism differs from that of other AA due to the loss of carbon via demethylation. If the molecule is subsequently remethylated, all the [^{15}N]-label is returned, but only a portion of [^{13}C] contained in the methyl group is returned due to dilution of that carbon in the methyl pool. The unlabeled demethylation (F_{nAADME}) and remethylation (F_{RMEnAA}) fluxes were calculated as

$$F_{nAADME} = Q_{nAA} \times k_{nAADME}, \quad [5]$$

and

$$F_{RMEnAA} = F_{nAADME} - F_{nAAIL}, \quad [6]$$

respectively, where k_{nAADME} is the mass-action rate constant for the n to methylation movement (per minute). The return of [^{13}C]-methyl carbon to the Met pool was predicted based on a polynomial fit to the [^{13}C]-Ser IR through time reflecting Ser acting as a substrate for the N^5-methyl-tetrahydrofolate pathway (IR_{Seri}; Finkelstein, 1990). Thus, the remethylation fluxes for the unlabeled, as well as the [^{13}C]- and [^{15}N]-labeled pools were represented as

$$F_{RMEnAAi} = F_{RMEnAA} \times IR_{Seri} \quad [7]$$

and

$$F_{RMEnAAii} = F_{RMEnAA} \times \frac{Q_{nAAii}}{Q_{nAA}}, \quad [8]$$

respectively. An example fit of the Ser IR over time is presented in Supplemental Figure S2 (https://doi.org/10.7294/24042825, Hruby et al., 2023).

Finally, instead of fitting the model solely to the 6 IR as previously undertaken (Yoder et al., 2020a), the model was fitted to the observed pool sizes of the 9 [^{13}C]-labeled, [^{15}N]-labeled, and unlabeled pools for extracellular, intracellular free, and intracellular bound plus the 6 IR for those pools. This change ensured that the predicted pool sizes were not of an inappropriate size and forced a more complete match of the model to the isotope data.

Model Initial Values

Inputs to the model were [^{15}N] IR for x (iIR_{xAAii}), n (iIR_{nAAii}), and p (iIR_{pAAii}); [^{13}C] IR for x (iIR_{xAAi}), n (iIR_{nAAi}) and p (iIR_{pAAi}); volumes of x (iV_x), n (iV_n), and p (iV_p); and concentrations of x (iC_x), n (iC_n), and p (iC_p). Each was calculated by AA and treatment using the mean of observations from the times 0 and 0.5 min. The second time point was found to not differ from time 0. Use of 6 observations from each treatment to set initial pool sizes yielded more stable estimates as compared with 3 values. Initial pool sizes and isotopic ratios are reported in Supplemental Table S3 (https://doi.org/10.7294/24042825, Hruby et al., 2023).

Model Fits

Each observation was randomly assigned to 1 of 3 experimental replicates by time point to yield 3 time series replicates for each treatment. This generated replicate represented the experimental unit for data analyses. The final time point, 240 min, was weighted 20 times relative to all other time points to help ensure that the model ended with the observed mass in each of the pools. Without the extra weight, the model often failed to replicate the last time point because it was the only time point after 60 min.

The *lsoda* method of the *ode* function from the deSolve software package was used to solve the series of differential equations (Soetaert et al., 2010). The

modCost and *modFit* functions of the FME package (Soetaert and Petzoldt, 2010) were used to generate residual errors and fit the model to each replicate by AA. The intracellular (n) pools were the mass drivers for all fluxes, but these pool sizes were very small compared to the extracellular and tissue-bound pools, which caused problems with optimization. This was addressed by setting *modCost* to scale residuals to the mean for each variable.

Model constants were estimated initially by AA and treatment using all of the data; that is, across replicates. The resulting predicted and observed values were used to identify outliers for removal based on studentized residuals: residuals/SD(residuals). Values greater than or equal to an absolute value of 4 were removed, and this equated to removal of 0% to 12.5% (3 points per treatment) of the data, respectively. Following outlier removal, the model was again fitted to the data across replicates to identify reasonable starting parameter estimates, followed by fits within each of the 3 replicates. The overall fit plus the 3-replicate fits were used for statistical analysis ($n = 3 + 1$). Data were plotted using the ggplot2 package (Villanueva and Chen, 2019). An example of fitted and observed data is displayed in Figure 2. The R code and corresponding data are available upon request.

Statistical Methods

Statistical analysis of AA concentrations, constant estimates, and fluxes was performed using the "stats" package (R Core Team, 2022) and the following linear model:

$$Y_{ij} = \mu + Val_i + NEAGG_j + (Val_i \times NEAAG_j) + \varepsilon_{ij}, \quad [9]$$

where Y_{ij} was the dependent variable, μ the population mean of Y, Val_i the fixed effect of Val (low or high), $NEAAG_j$ the fixed effect of NEAAG (low or high), and $Val_i \times NEAAG_j$ the interaction of Val and NEAAG. Outliers were removed if absolute values of studentized residuals were greater than 3. Using this criterion, none or a single outlier was removed from each AAx treatment depending on the factor. Removal of 1 outlier represented approximately 6% of the data.

In addition, concordance correlation coefficients (**CCC**) and root mean square errors as a percentage of the mean (**RMSE**) for IR_{nKAii} and IR_{Seri} were calculated for each AA using the epiR package. The CCC provides a dimensionless evaluation of precision and accuracy (Lin, 1989), and RMSE reflects the mean variance around the line of unity between the predicted and observed data (Bibby and Toutenburg, 1977). Typically CCC scores below 0.50 or RMSE greater than 40% are deemed of poor quality (Yoder et al., 2021), but these fit quality standards were not used to drive outlier removal.

RESULTS AND DISCUSSION

Media Concentrations

Measured concentrations and IR of [^{15}N]-AA and [^{13}C]-AA in treatment media are displayed in Table 1 and Table 2, respectively. Deviations in observed concentrations relative to target values in [^{13}C]-labeled media were greater than for the [^{15}N]-labeled media. We attribute this to the smaller volume of [^{13}C]-labeled AA media prepared; thus, smaller volumes of the AA stocks were pipetted, resulting in greater preparation error. However, the desired treatment differences were achieved for Ala, Gln, Gly, and Val (Supplemental Table S4; https://doi.org/10.7294/24042825, Hruby et al., 2023). The AA concentrations in [^{15}N]-labeled and [^{13}C]-labeled algae purchased from Cambridge Isotope Laboratories Inc. varied by AA (Yoder et al., 2020a), resulting in an atom percent enrichment (AP) ranging from 19% to 92% depending on treatment. All other AA remained constant across treatments. Over the 8-h period between media changes, concentrations for most AA decreased by approximately 50% (Supplemental Table S5; https://doi.org/10.7294/24042825, Hruby et al., 2023).

Model Fit Quality

The CCC and RMSE for IR_{nKAii} and IR_{Seri} are reported in Supplemental Table S6 (https://doi.org/10.7294/24042825, Hruby et al., 2023). In addition, the CCC and RMSE for the fitted models for all 15 fitted pools and IR for each AA are displayed in Supplemental Table S7 (https://doi.org/10.7294/24042825, Hruby et al., 2023). Overall, fits for IR_{nKAii} and IR_{Seri} were accurate and precise (CCC from 0.6 to 0.97; RMSE <12% of the mean). The CCC values for Q_{pAA} could not be reported because $F_{nAAtfAA}$ was set equal to $F_{tfAAnAA}$, yielding no variance in predicted pool sizes. The CCC values for IR_{pAAii} and Q_{pAAii} were low for all AA, although these data appeared to be flat, which was captured in the model. In contrast, the CCC values were moderate for IR_{pAAi} and Q_{pAAi}, except for Ala, where values were close to 0. Interestingly, this was not observed by Yoder et al. (2021), which was likely due to the shorter observational period in that study. When compared without the last time point, the pattern was identical to that reported previously. The model was unable to capture the IR increase up to 1 h

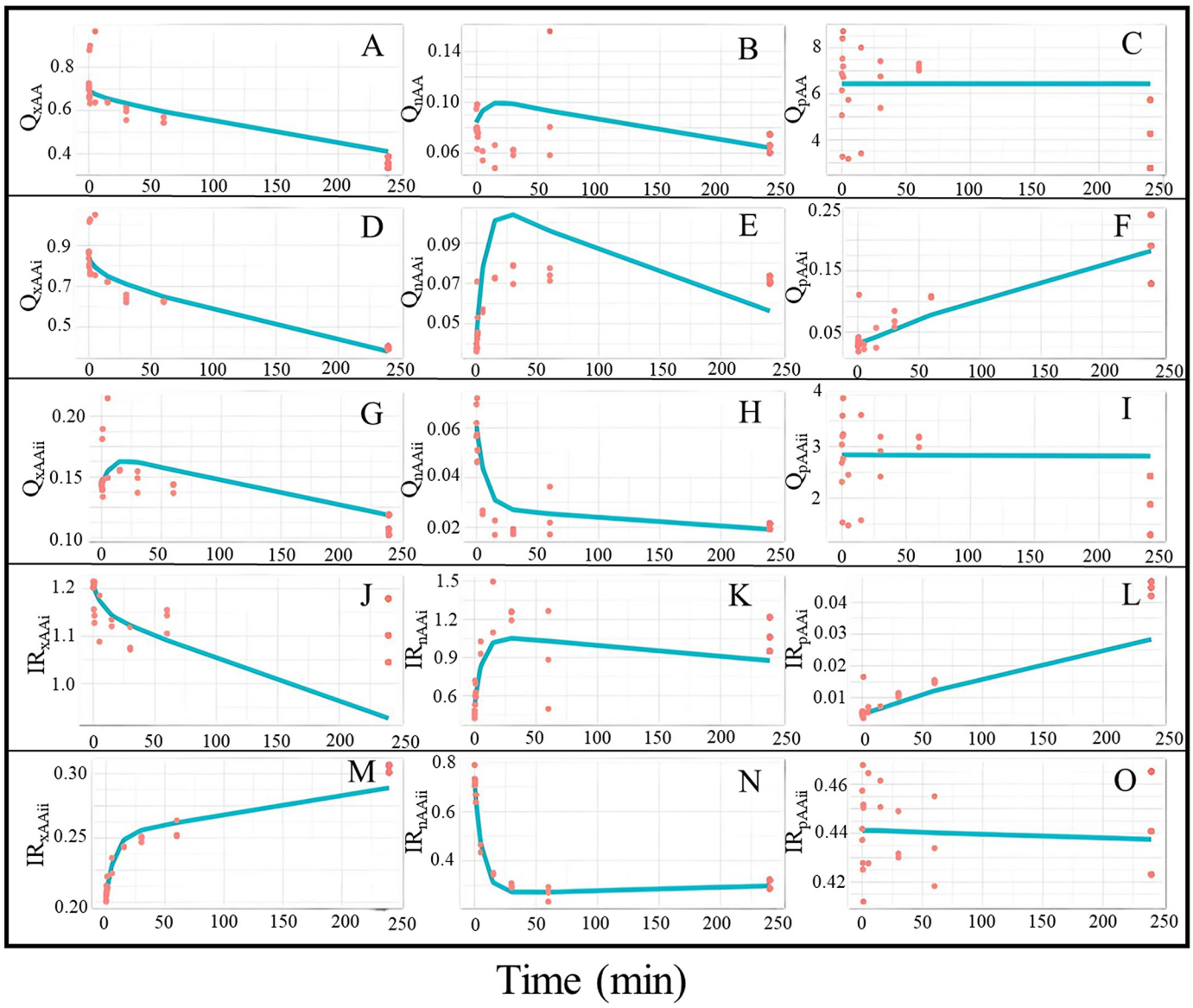

Figure 2. Example of model fit with observed (red dots) and predicted (blue line): (A) Q_{xAA} = unlabeled extracellular Leu pool (μmol); (B) Q_{nAA} = unlabeled intracellular free Leu pool (μmol); (C) Q_{pAA} = unlabeled intracellular bound- Leu pool; (D) Q_{xAAi} = [^{13}C]-labeled extracellular AA pool (μmol); (E) Q_{nAAi} = [^{13}C]-labeled intracellular free Leu pool (μmol); (F) Q_{pAAi} = [^{13}C]-labeled intracellular bound AA pool (μmol); (G) Q_{xAAii} = [^{15}N]-labeled extracellular free Leu pool (μmol); (H) Q_{nAAii} = [^{15}N]-labeled intracellular free Leu pool (μmol); (I) Q_{pAAii} = [^{15}N]-labeled intracellular bound Leu pool (μmol); (J) IR_{xAAi} = extracellular isotope ratio (IR) of [^{13}C] to [^{12}C]; (K) IR_{nAAi} = intracellular IR of [^{13}C] to [^{12}C]; (L) IR_{pAAi} = intracellular bound IR of [^{13}C] to [^{12}C] (M) IR_{xAAii} = extracellular IR of [^{15}N] to [^{12}C]; (N) IR_{nAAii} = intracellular IR of [^{15}N] to [^{12}C]; (O) IR_{pAAii} = intracellular bound IR of [^{15}N] to [^{12}C].

and the following decline. In addition, Met had the lowest CCC and highest RMSE for all fits. This is probably due to very low media concentrations, which increased the relative error.

Fluxes and Concentrations of BCAA

Fluxes for the BCAA are reported in Table 3 and depicted in Figure 3. As expected, net uptake of Val increased for the HVal treatments ($P < 0.001$), but an interaction also occurred between NEAAG and Val ($P = 0.04$), with an increased difference between LVal and HVal treatments with HNEAAG. Net uptake of Leu and Ile was also significantly decreased by the HVal treatment ($P < 0.01$ and $P < 0.01$, respectively).

Medium AA concentrations were the most important controlled contributor to uptake and release of Val. Influx of Val (F_{xAAnAA}) increased approximately 400%

Table 2. Mean unlabeled AA concentrations (Conc; μM), SD,[1] and isotope ratios (IR)[2] by treatment[3] in the [^{13}C]-labeled extracellular media before cell exposure

	Treatment											
	LNEAAG, LVal			LNEAAG, HVal			HNEAAG, LVal			HNEAAG, HVal		
AA	Conc	SD	IR	Conc	SD	IR	Conc	SD	IR	Conc	SD	IR
Ala	90.6	7.95	2.08	81.1	1.46	2.18	443	18.4	0.43	501	29.2	0.43
Arg	48.0	2.32	0.73	45.2	0.40	0.75	43.2	1.72	0.76	51.8	4.00	0.66
Asp	5.50	2.01	11.9	5.60	1.36	11.0	5.47	1.51	10.9	5.35	1.79	12.6
Gln	27.6	14.4	1.35	28.6	11.9	1.34	64.8	41.2	1.34	96.0	42.1	1.34
Glu	65.0	11.0	1.64	57.6	5.36	1.74	71.1	17.5	1.40	68.9	20.3	1.61
Gly	182	22.9	—	182	25.6	—	564	23.0	—	664	32.5	—
His	34.2	1.19	2.67	29.3	2.26	2.90	29.0	1.90	2.88	35.2	4.81	2.52
Ile	61.0	3.79	1.60	57.4	1.71	1.60	54.0	2.78	1.63	63.6	3.10	1.54
Leu	128	8.43	1.20	118	2.36	1.22	112	4.67	1.22	130	9.04	1.18
Lys	41.2	5.06	0.84	39.5	0.58	0.84	37.5	3.73	0.81	45.5	3.68	0.76
Met	6.67	0.98	5.99	6.65	0.58	5.87	6.32	1.04	6.04	7.25	0.71	5.59
Phe	9.33	1.86	15.3	8.63	0.54	16.2	7.89	0.24	17.0	7.94	0.11	18.7
Pro	85.7	5.19	0.50	78.5	2.08	0.51	75.5	3.02	0.51	86.5	4.78	0.50
Ser	66.8	4.79	0.72	62.2	1.03	0.73	59.2	1.78	0.73	67.2	3.20	0.72
Thr	31.0	3.08	3.31	28.7	0.62	3.47	27.7	0.73	3.39	30.2	1.76	3.29
Tyr	2.37	0.09	4.71	2.09	0.24	4.87	2.10	0.19	4.69	2.86	0.16	4.12
Val	141	7.44	0.91	530	11.8	0.23	126	4.57	0.91	558	8.59	0.22

[1]Representative of 3 samples.

[2]IR = $\frac{^{13}C}{^{12}C}$.

[3]LNEAAG = low nonessential AA group (70% of in vivo concentrations of Ala, Gln, and Gly); HNEAAG = high nonessential AA group (200% in vivo concentrations of Ala, Gln, and Gly); LVal = low Val (70% of in vivo concentration); HVal = high Val (200% of in vivo concentration).

with HVal compared with LVal ($P < 0.001$; Table 3), and the response was not dependent on NEAAG concentrations. The extra Val apparently exceeded anabolic needs as intracellular free concentrations rose to more than 200% of LVal (Table 4). This contributed to approximately a 300% increase in efflux from the cell (F_{nAAxAA}), a 200% increase in transamination (F_{nAAnKA}), and a 200% increase in irreversible loss (F_{nAAIL}) of Val. The error was high for the flux into bound protein ($F_{nAAtfAA}$), resulting in no treatment differences, but the flux numerically increased from LVal to HVal by approximately 200%. This nonsignificant effect is supported by significant increases in intracellular bound concentrations of Val with HVal ($P = 0.04$; Table 5). None of these responses was significantly affected by the NEAAG treatment.

Uptake and efflux of Leu and Ile behaved slightly differently. Influx (F_{xAAnAA}) and efflux (F_{nAAxAA}) of Leu increased with HNEAAG ($P < 0.01$; Table 3), and Ile tended to increase with HVal ($P = 0.06$). The increase in efflux of Leu could explain the decreased net uptake of Leu with HVal concentrations. Interestingly, these effects do not seem to be due to mass-action Leu effects because intracellular free concentrations decreased with HNEAAG ($P < 0.01$). Increased transporter activity (most likely System L transporters, although others could have also contributed), was apparently caused by high intracellular concentrations of Ala and Gly, which would drive greater exchange rates that were not associated with Val concentrations (further discussed below).

Influx (F_{xAAnAA}) and efflux (F_{nAAxAA}) of Ile were affected by the interaction of NEAAG and Val ($P < 0.001$ and $P < 0.01$, respectively; Table 3), with Ile influx rates being the greatest for the HNEAAG plus LVal treatment, which could be attributed to increased transporter activity caused by an increased supply of NEAAG and decreased competition from Val.

Transamination (F_{nAAnKA}) of Ile and Leu decreased in the presence of HVal ($P = 0.04$ and $P < 0.001$, respectively; Table 3). To our knowledge, there have been no comparative studies measuring the effects of HVal on transamination, but 1.0 mmol/L of Leu decreased transamination of Val by 48% in perfused rat hearts (Torres et al., 1995). High Val tended to reduce the irreversible loss (F_{nAAIL}) of Ile and Leu with HNEAAG ($P = 0.06$ and $P = 0.08$, respectively). It is unlikely that these effects were due to mass action because the intracellular concentrations of Ile and Leu did not change with Val treatment (Table 4; Table 5). Removal of BCAA in excess of milk-protein-synthesis needs, which resulted in catabolism and transfer of the released N to NEAA, has been previously observed (Wohlt et al., 1977; Hanigan et al., 2001, 2002).

Table 3. Bovine mammary epithelial cell amino acid flux rates (nmol/min) in response to varying media concentrations of Val and Ala, Gln, and Gly (NEAAG)[1]

	LNEAAG		HNEAAG			*P*-value		
Item	LVal	HVal	LVal	HVal	SEM	NEAAG	Val	NEAAG × Val
Ala								
Net uptake	−3.14[ab]	−11.2[b]	3.89[a]	7.20[a]	3.06	<0.01	0.38	0.09
F_{xAAnAA}	18.2	35.2	49.2	69.0	11.9	0.02	0.15	0.91
F_{nAAxAA}	21.3	46.4	45.3	61.8	12.7	0.17	0.13	0.74
F_{nAAnKA}	171	143	239	328	60.4	0.06	0.62	0.35
F_{nKAnAA}	56.4	42.1	80.2	73.0	13.3	0.06	0.43	0.79
$F_{nAAtfAA}$	0.801	0.799	1.79	4.29	0.87	0.04	0.21	0.18
F_{nAAIL}	114	101	159	172	36.7	0.15	0.97	0.73
$F_{Synthesis}$	130	105	161	180	43.0	0.25	0.91	0.62
Ile								
Net uptake	1.41[a]	0.424[b]	1.21[a]	0.803[ab]	0.179	0.76	<0.01	0.13
F_{xAAnAA}	2.15[b]	4.15[ab]	5.68[a]	2.32[b]	0.553	0.29	0.41	<0.001
F_{nAAxAA}	0.738[b]	3.73[a]	2.68[ab]	1.52[ab]	0.628	0.73	0.11	<0.01
F_{nAAnKA}	0.669	0.638	0.729	0.499	0.059	0.49	0.04	0.12
F_{nKAnAA}	0.060	0.008	0.040	0.016	0.019	0.62	0.09	0.48
$F_{nAAtfAA}$	0.237	0.287	0.312	0.333	0.031	0.08	0.26	0.67
F_{nAAIL}	0.610	0.629	0.689	0.483	0.054	0.56	0.08	0.06
Leu								
Net uptake	2.64[a]	1.33[b]	2.25[ab]	1.17[b]	0.303	0.38	<0.01	0.70
F_{xAAnAA}	5.63[b]	9.11[ab]	11.46[a]	11.33[a]	1.08	<0.01	0.18	0.12
F_{nAAxAA}	2.98[b]	7.81[ab]	9.21[a]	10.15[a]	1.31	<0.01	0.06	0.17
F_{nAAnKA}	1.35[a]	1.15[ab]	1.33[a]	0.924[b]	0.067	0.07	<0.001	0.16
F_{nKAnAA}	0.108	0.014	0.047	0.014	0.024	0.15	0.03	0.24
$F_{nAAtfAA}$	0.651	0.728	0.699	0.766	0.050	0.46	0.17	0.92
F_{nAAIL}	1.24[a]	1.13[ab]	1.29[a]	0.910[b]	0.067	0.17	<0.01	0.08
Met								
Net uptake	0.158	0.108	0.103	0.119	0.025	0.48	0.58	0.22
F_{xAAnAA}	0.258	0.173	0.149	0.167	0.033	0.15	0.38	0.15
F_{nAAxAA}	0.048[ab]	0.046[b]	0.065[ab]	0.100[a]	0.011	0.01	0.21	0.14
F_{nAADME}	0.075	0.075	0.054	0.038	0.018	0.14	0.67	0.65
F_{RMEnAA}	0.004	0.036	0.024	0.001	0.015	0.76	0.89	0.09
$F_{nAAtfAA}$	0.016	0.009	0.034	0.021	0.011	0.20	0.41	0.79
$F_{DMEAAIL}$	0.071	0.014	0.030	0.036	0.014	0.52	0.10	0.04
Phe								
Net uptake	−1.98	−0.92	−0.71	−1.79	0.52	0.48	0.70	0.07
F_{xAAnAA}	1.10[b]	1.01[b]	1.72[ab]	2.84[a]	0.29	<0.01	0.13	0.06
F_{nAAxAA}	3.08	1.92	2.44	4.24	0.80	0.32	0.69	0.09
F_{nAAnKA}	0.04[b]	0.02[b]	0.02[b]	0.14[a]	0.02	<0.01	0.02	<0.01
F_{nKAnAA}	0.01	0.01	0.06	0.10	0.03	0.04	0.52	0.54
$F_{nAAtfAA}$	0.95	0.53	0.40	0.36	0.11	<0.01	0.05	0.12
F_{nAAIL}	0.03	0.00	0.00	0.06	0.02	0.51	0.23	0.03
Thr								
Net uptake	43.0	41.6	45.4	59.4	11.6	0.40	0.59	0.52
F_{xAAnAA}	48.8	50.4	58.0	65.0	12.3	0.35	0.73	0.83
F_{nAAxAA}	5.84	8.83	9.52	5.55	1.81	0.97	0.90	0.08
F_{nAAnKA}	0.589[ab]	0.749[a]	0.522[ab]	0.375[b]	0.088	0.02	0.85	0.11
F_{nKAnAA}	0.189	0.326	0.200	0.204	0.066	0.43	0.28	0.34
$F_{nAAtfAA}$	0.298	0.161	0.187	0.319	0.061	0.71	0.97	0.05
F_{nAAIL}	0.401	0.423	0.322	0.170	0.071	0.03	0.43	0.25
Val								
Net uptake	2.34[b]	5.18[a]	1.14[b]	6.11[a]	0.444	0.30	<0.001	0.04
F_{xAAnAA}	6.74[b]	27.6[b]	9.38[b]	31.5[a]	2.69	0.55	<0.001	0.82
F_{nAAxAA}	4.40[b]	22.4[a]	8.24[b]	25.3[a]	2.84	0.46	<0.001	0.88
F_{nAAnKA}	1.36[b]	3.61[a]	1.44[b]	3.71[a]	0.241	0.33	<0.001	0.97
F_{nKAnAA}	0.122[b]	0.279[a]	0.071[b]	0.287[a]	0.032	0.28	<0.001	0.38
$F_{nAAtfAA}$	3.19	12.4	3.48	11.1	7.63	0.95	0.29	0.92
F_{nAAIL}	1.24	3.33	1.37	3.35	0.23	0.34	<0.001	0.82

[a,b]Letters denote a Tukey means separation test. Least squares means within rows with no common superscripts differ ($P \leq 0.05$).

[1]Data are presented as least squares means. LNEAAG = low nonessential AA group (70% of in vivo concentrations of Ala, Gln, and Gly); HNEAAG = high nonessential AA group (200% of in vivo concentrations of Ala, Gln, and Gly); LVal = low Val (70% of in vivo concentration); HVal = high Val (200% of in vivo concentration). $F_{Synthesis}$ = amino acid synthesis rate (nmol/min), net uptake = flux of extracellular to intracellular free AA minus flux of intracellular free AA to extracellular AA (nmol/min); F_{xAAnAA} = flux of extracellular to intracellular free AA, F_{nAAxAA} = intracellular free to extracellular AA (nmol/min), F_{nAAnKA} = flux of intracellular free AA to transamination (nmol/min), F_{nKAnAA} = rate of reamination (nmol/min), $F_{nAAtfAA}$ = intracellular free AA to tissue fast protein synthesis (nmol/min), F_{nAAIL} = flux of the percentage of transaminated AA subjugated to irreversible loss (nmol/min), F_{nAADME} = rate of intracellular free AA to demethylation of Met (nmol/min), $FRME_{nAA}$ = rate of remethylation of Met (nmol/min).

Rate Constants for BCAA

To unravel the potential causes of the flux changes discussed in the prior section, one must evaluate the kinetic constants. With only 2 concentrations of each factor, such an evaluation is restricted to assessment of mass-action effects. Mass-action kinetics are characterized as a linear relationship between substrate concentrations and the rate of activity (Horn and Jackson, 1972), and changes in the constants reflect altered enzyme affinity, capacity, or saturation of activity (López et al., 2006).

Of the 4 L-type amino acid transporters (**LAT**) System L transporters, 3 are known to be expressed in bovine mammary glands: LAT1, LAT2, and LAT3 (Baik et al., 2009; Fu et al., 2021), and LAT4 has been found in the endometria of beef cattle (Forde et al., 2014; França et al., 2017). System L transporters use an exchange mechanism to concentrate AA in the cell (Christensen, 1990) with 1 mol of AA transported across the cell membrane for each mole of AA transported across the membrane in the opposite direction. The exchange of AA is one for which the transporter has affinity, and when in high concentrations within the cells relative to extracellularly, it generates motive force. Motive force is often achieved via active transport catalyzed by Na-dependent transporters. Because Na-dependent transporters typically transport smaller AA, the NEAA are concentrated within the cells, driving influx of other System L AA and allowing them to be concentrated inside the cell.

Mass-action constants are presented in Table 6. Valine concentrations had no significant effects on the influx or efflux rate constants for Val transport, indicating that the flux changes with Val treatment were driven solely by mass action. However, Val transporter activity was stimulated by HNEAAG, which is reflected in the increased influx and efflux rate constant estimates ($P < 0.01$ and $P < 0.001$, respectively; Table 6). This presumably reflects the effects of increased intracellular concentrations of NEAAG and not a change in the amount of transporter present. To rule out the possibility of saturation effects, a total BCAA kinetic curve was generated for uptake by fitting a logarithmic equation to the summed concentration and uptake velocity data of Yoder et al. (2021). Summation of the same for the HVal treatment herein indicated that the transporter was operating at approximately half-maximal velocity and therefore definitely not saturated. Thus, we can conclude that herein, the activation of transport activity was due to the intracellular substrate effects of HNEAAG acting on System L.

It is interesting to note that Val, but not Ile or Leu, is also transported with low affinity by the Na-dependent Ala, Ser, and Cys (**ASC**) transporter system that is shared by all 3 of the NEAA in NEAAG (Arriza et al., 1993). However, because HNEAAG activated Val transport rather than inhibited it, the primary mechanism for Val transport must be System L exchange transporters and not competitive inhibition at the ASC transporters.

Transporter activity is known to increase and decrease with low and high concentrations of homologous AA, respectively. For example, System A sodium-coupled neutral amino acid transporter 2 (**SNAT2**), which transports mainly Ala and Gln, increased by 20-fold when rat mammary gland explants were incubated in media without AA (López et al., 2006; Bröer and Bröer, 2017). The same transporter was downregulated in response to increasing total AA concentrations in porcine MEC (Chen et al., 2018). The lack of changes in BCAA transport in response to changing Val concentrations ($P > 0.05$) suggests that adaptive mechanisms controlling System L in bovine MEC make a minor contribution to overall transport of the BCAA within normal biological ranges. Greater changes in extracellular concentrations may be required to stimulate changes in activity. However, there were significant interactions of Val and NEAAG for the influx parameters of both Leu and Ile.

The influx constants for Ile and Leu were highest with LVal plus HNEAAG, indicating reduced competition by Val and the substrate effects of intracellular HNEAAG (Table 6). In contrast, LNEAAG plus HVal caused a 90% increase in the influx constants for Ile and Leu compared with LNEAAG plus LVal, which was not the case for Val. This result was the opposite of what we expected. This may reflect stimulation of other BCAA transporters or a modification of System L to increase affinity for Ile and Leu to maintain intracellular concentrations of the latter. For Leu, it could also be due to stimulation of the $b^{0,+}$ (Chillarón et al., 1996) and y^+L (Pfeiffer et al., 1999) transporter systems, which act on Leu, but not Ile and Val.

The Leu efflux rate constant increased with HNEAAG at both Val concentrations, but the effect had an interaction for Ile (Table 6). Given that System L transporters are bidirectional (Verrey, 2003), HNEAAG in the media would be expected to cause greater efflux of the BCAA from the cells as a result of NEAA substrate effects. Additionally, influx of the BCAA would also be expected to increase due to greater intracellular concentrations of the NEAA resulting from Na-linked transport.

However, for both Leu and Ile, LVal coupled with HNEAAG resulted in the highest influx constants, reflecting reduced competition from Val and increased exchange AA availability within the cell (Table 6).

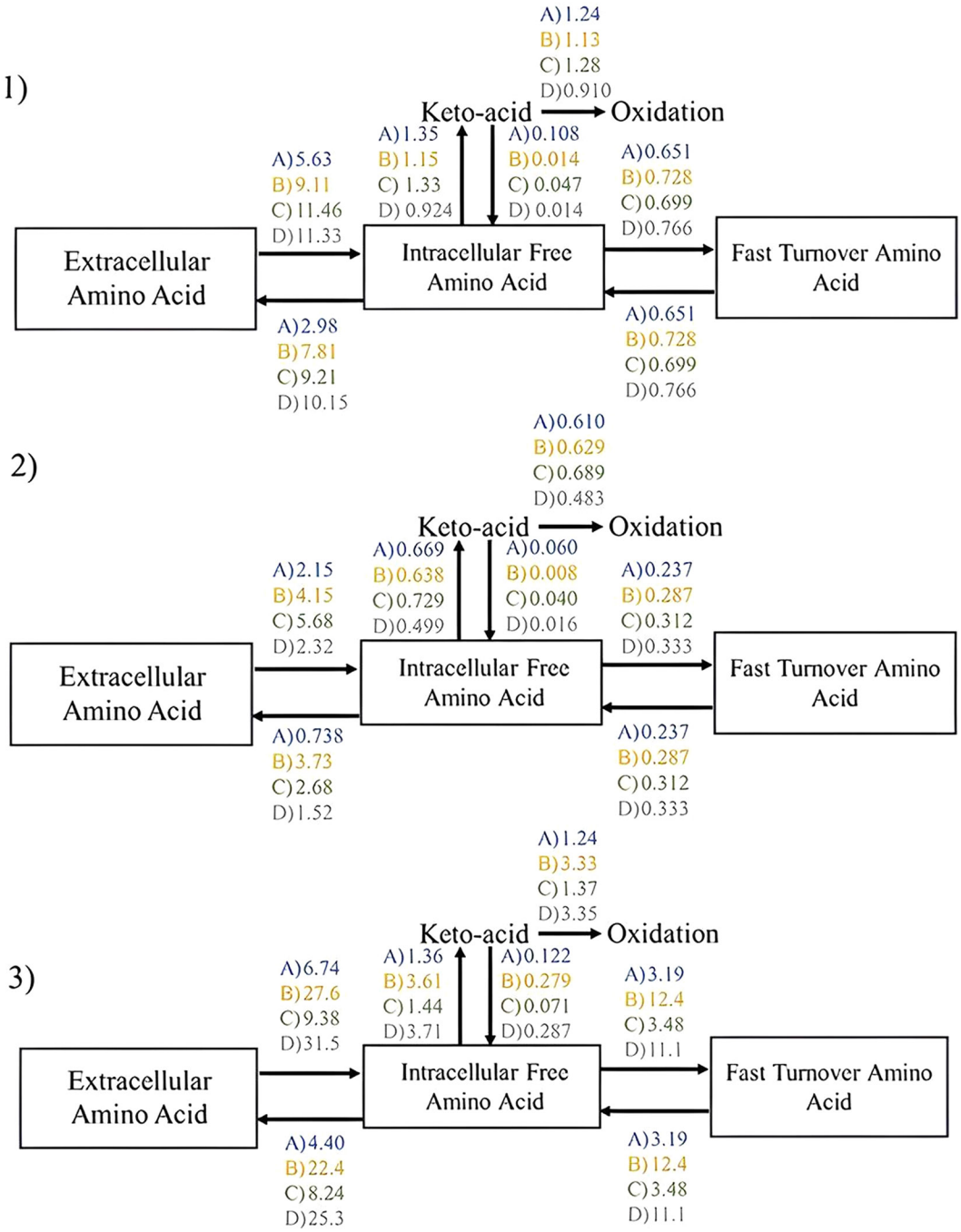

Figure 3. Schematic of a bovine mammary epithelial cell model for unlabeled (1) leucine, (2) isoleucine, and (3) valine, with boxes representing pools and arrows representing fluxes. The fluxes depicted are in nanomoles per minute with the following treatments: (A) low valine, low alanine, glutamine, and glycine (blue); (B) high valine, low alanine, glutamine, and glycine (gold); (C) low valine, high alanine, glutamine, and glycine (green); and (D) high valine, high alanine, glutamine, and glycine (gray).

With HNEAAG, HVal caused a 68% drop in Ile and only a 15% drop in Leu for the influx rate constant, suggesting competitive inhibition that affects Ile and Leu to varying degrees. System L transporter LAT1 is highly expressed in bovine mammary cells (Lin et al., 2018), and it has the highest affinity for Leu followed by Ile and Val (Kanai et al., 1998; Yanagida et al., 2001). This could explain the greater decline in the influx constant for Ile as compared with Leu in response to HVal plus HNEAAG.

The greater affinity for Leu may also explain the increase in both influx and efflux constants with

Table 4. Effect of treatment and time (min) on total intracellular free AA concentrations (μ*M*) in bovine mammary epithelial cells after addition of [^{13}C]-labeled treatment media[1]

	LNEAAG		HNEAAG			*P*-value			
AA	LVal	HVal	LVal	HVal	SEM	NEAAG	Val	NEAAG × Val	Time
Ala	2,304	2,064	2,979	2,832	195	<0.01	0.24	0.81	0.53
Arg[2]	86.0	82.9	69.0	75.6	12.9	0.35	0.88	0.71	0.90
Asp	458	451	430	428	34.7	0.37	0.98	0.94	<0.01
Gln[2]	1,523	2,372	4,830	3,708	1,225	0.07	0.94	0.42	0.20
Glu	1,474	1,461	1,325	1,338	96.6	0.15	0.93	0.89	0.22
Gly[3]	1,853	1,683	2,451	2,436	133	<0.01	0.43	0.56	0.20
His[2]	370	289	235	206	25.6	<0.01	0.04	0.31	0.87
Ile	199	217	176	195	12.9	0.09	0.21	0.97	0.29
Leu	323	387	311	322	25.0	<0.01	0.79	0.60	0.35
Lys	99.0	142	81.1	87.6	19.7	0.07	0.23	0.36	0.34
Met	156	149	131	126	9.32	<0.01	0.60	0.88	0.04
Phe	199	182	146	147	14.4	<0.01	0.46	0.53	0.23
Pro	1,229	1,079	772	752	79.8	<0.01	0.26	0.42	0.76
Ser	729	691	665	659	52.2	0.32	0.47	0.76	<0.01
Thr	567	478	386	375	28.3	<0.01	0.06	0.18	0.16
Tyr	49.7	44.8	40.6	32.8	4.67	0.04	0.19	0.76	<0.01
Val	454	1,081	344	869	51.4	<0.01	<0.01	0.33	0.01

[1]Data are presented as least squares means. LNEAAG = low nonessential AA group (70% of in vivo concentrations of Ala, Gln, and Gly); HNEAAG = high nonessential AA group (200% of in vivo concentrations of Ala, Gln, and Gly); LVal = low Val (70% of in vivo concentration); HVal = high Val (200% of in vivo concentration).

[2]No [^{15}N] isotope present for AA.

[3]Unable to differentiate [^{15}N] or [^{13}C] isotope present for AA.

HNEAAG ($P < 0.001$ and $P = 0.02$, respectively; Table 6). Leucine may be more responsive to NEAAG as compared with Ile due to Leu being transported by more than one exchange transporter (System L and System y^+L).

Transamination and irreversible-loss rate constants (k_{nAAnKA} and k_{nKAIL}) of all 3 BCAA were decreased with high concentrations of Val (Table 6), indicating either downregulation or partial saturation of the BCAA transaminase and branched-chain α-keto acid dehydrogenase

Table 5. Effect of treatment and time (min) on total intracellular bound AA concentrations (m*M*) in bovine mammary epithelial cell protein pellets after addition of [^{13}C]-labeled treatment media[1]

	LNEAAG		HNEAAG			*P*-value			
AA	LVal	HVal	LVal	HVal	SEM	NEAAG	Val	NEAAG × Val	Time
Ala	50.0	51.8	57.2	58.2	1.20	<0.01	0.26	0.74	0.10
Arg[2]	48.9	47.9	53.7	52.0	4.58	0.36	0.80	0.94	0.27
Asp	74.3	76.2	77.0	79.3	1.99	0.15	0.23	0.91	<0.01
Gln[2]	17.2	15.8	11.4	15.2	2.15	0.13	0.54	0.24	0.30
Glu	57.3	59.4	59.3	59.5	1.80	0.51	0.48	0.61	0.17
Gly[3]	21.9	21.8	28.5	29.7	0.76	<0.01	0.52	0.41	0.12
His[2]	13.4	14.2	14.3	14.9	0.42	0.07	0.11	0.79	0.27
Ile	31.7	33.5	32.9	33.7	1.23	0.59	0.19	0.67	0.13
Leu	68.4	71.8	70.6	71.2	2.38	0.76	0.28	0.55	0.11
Lys	63.6	66.1	64.9	65.7	2.39	0.86	0.26	0.73	<0.01
Met	17.3	17.8	17.1	17.2	0.51	0.44	0.40	0.73	<0.01
Phe	27.2	27.7	26.5	27.7	0.68	0.62	0.10	0.67	<0.01
Pro	42.2	43.5	43.5	43.2	1.44	0.73	0.53	0.58	0.09
Ser	27.6	28.4	30.4	31.5	0.89	<0.01	0.30	0.91	0.31
Thr	26.0	25.7	24.4	25.0	0.72	0.14	0.61	0.56	<0.01
Tyr	14.8	14.7	14.6	14.4	0.37	0.42	0.72	0.97	0.05
Val	45.2	49.8	46.7	50.0	1.96	0.63	0.04	0.74	0.40

[1]Data are presented as least squares means. LNEAAG = low nonessential AA group (70% of in vivo concentrations of Ala, Gln, and Gly); HNEAAG = high nonessential AA group (200% of in vivo concentrations of Ala, Gln, and Gly); LVal = low Val (70% of in vivo concentration); HVal = high Val (200% of in vivo concentration).

[2]No [^{15}N] isotope present for AA.

[3]Unable to differentiate ^{15}N or ^{13}C isotope present for AA.

Table 6. Amino acid transport and metabolism rate constants (per minute) of bovine mammary epithelial cells in response to varying media concentrations of Val and Ala, Gln, and Gly (NEAAG)[1]

	LNEAAG		HNEAAG			*P*-value		
Item	LVal	HVal	LVal	HVal	SEM	NEAAG	Val	NEAAG × Val
Ala								
k_{xAAnAA}	0.026[a]	0.027[a]	0.016[b]	0.016[b]	0.002	<0.001	0.82	0.86
k_{nAAxAA}	0.041	0.051	0.041	0.041	0.006	0.41	0.44	0.48
$k_{nAAtfAA}$	0.0005	0.0004	0.0006	0.0011	0.0006	0.54	0.71	0.65
k_{nAAnKA}	0.377	0.208	0.274	0.283	0.075	0.85	0.31	0.26
k_{nKAIL}	0.258	0.143	0.191	0.205	0.053	0.96	0.36	0.24
$k_{synthesis}$	0.145	0.071	0.191	0.144	0.042	0.17	0.18	0.75
Ile								
k_{xAAnAA}	0.008[b]	0.015[ab]	0.022[a]	0.007[b]	0.002	0.29	0.20	<0.001
k_{nAAxAA}	0.018	0.084	0.068	0.032	0.017	0.85	0.29	0.01
$k_{nAAtfAA}$	0.006	0.006	0.007	0.008	0.0008	0.09	0.91	0.74
k_{nAAnKA}	0.018	0.013	0.018	0.011	0.002	0.42	<0.01	0.55
k_{nKAIL}	0.016	0.013	0.017	0.010	0.002	0.50	0.01	0.38
Leu								
k_{xAAnAA}	0.007[b]	0.013[ab]	0.020[a]	0.017[a]	0.002	<0.001	0.40	0.04
k_{nAAxAA}	0.024[b]	0.102[ab]	0.113[a]	0.122[a]	0.021	0.02	0.06	0.11
$k_{nAAtfAA}$	0.008	0.007	0.008	0.010	0.0009	0.19	0.67	0.19
k_{nAAnKA}	0.017[a]	0.012[b]	0.016[ab]	0.010[c]	0.001	0.11	<0.001	0.82
k_{nKAIL}	0.016[a]	0.011[ab]	0.016[ab]	0.010[b]	0.001	0.27	0.001	0.55
Met								
k_{xAAnAA}	0.006	0.004	0.003	0.004	0.0009	0.18	0.60	0.26
k_{nAAxAA}	0.014	0.010	0.007	0.008	0.002	0.05	0.42	0.12
$k_{nAAtfAA}$	0.002	0.001	0.004	0.002	0.0009	0.11	0.18	0.69
k_{nAADME}	0.011	0.011	0.008	0.007	0.003	0.22	0.87	0.81
k_{DMEIL}	0.011	0.002	0.005	0.007	0.002	0.90	0.22	0.06
Phe								
k_{xAAnAA}	0.017	0.017	0.036	0.041	0.008	0.02	0.70	0.76
k_{nAAxAA}	0.199	0.104	0.146	0.195	0.055	0.77	0.61	0.21
$k_{nAAtfAA}$	0.063[a]	0.025[ab]	0.020[b]	0.018[b]	0.010	0.03	0.06	0.11
k_{nAAnKA}	0.0005[b]	0.0005[b]	0.0005[b]	0.0006[a]	0.00001	<0.001	<0.001	<0.001
k_{nKAIL}	0.0015	0.0004	5.6×10^{-9}	0.003	0.001	0.60	0.52	0.07
Thr								
k_{xAAnAA}	0.021	0.028	0.038	0.022	0.007	0.53	0.55	0.11
k_{nAAxAA}	0.049	0.078	0.130	0.075	0.021	0.12	0.65	0.07
$k_{nAAtfAA}$	0.002	0.0006	0.001	0.004	0.0008	0.19	0.68	0.04
k_{nAAnKA}	0.003	0.005	0.004	0.002	0.001	0.28	0.98	0.09
k_{nKAIL}	0.003	0.004	0.004	0.002	0.0008	0.48	0.34	0.12
Val								
k_{xAAnAA}	0.008[ab]	0.008[b]	0.014[a]	0.013[ab]	0.001	<0.01	0.62	0.58
k_{nAAxAA}	0.032[b]	0.050[b]	0.078[a]	0.081[a]	0.008	<0.001	0.21	0.35
$k_{nAAtfAA}$	0.004[a]	0.002[b]	0.006[a]	0.004[ab]	0.0007	0.04	<0.01	0.60
k_{nAAnKA}	0.013[a]	0.008[b]	0.013[a]	0.009[b]	0.001	0.95	<0.001	0.64
k_{nKAIL}	0.012[a]	0.007[b]	0.012[a]	0.008[ab]	0.001	0.77	0.001	0.93

[a,b]Letters denote a Tukey means separation test. Least squares means within rows with no common superscripts differ ($P \leq 0.05$).

[1]Data are presented as least squares means. LNEAAG = low nonessential AA group (70% of in vivo concentrations of Ala, Gln, and Gly); HNEAAG = high nonessential AA group (200% of in vivo concentrations of Ala, Gln, and Gly); LVal = low Val (70% of in vivo concentration); HVal = high Val (200% of in vivo concentration). $k_{synthesis}$ = rate of amino acid synthesis (per minute), k_{xAAnAA} = constant estimate for extracellular AA to intracellular free AA pools (per minute), k_{nAAxAA} = constant estimate for intracellular free AA to extracellular AA (per minute), $k_{nAAtfAA}$ = intracellular free AA to fast protein synthesis (per minute), k_{nAAnKA} = transamination constant (per minute), k_{nAADME} = constant estimate for intracellular free AA to methylated AA (min-1), $k_{nKAIL} = f_{nKAIL}$ (fractional irreversible loss in percent divided by 100) × k_{nAAnKA}, $k_{DMEIL} = f_{DMEIL}$ (fractional irreversible loss in percent divided by 100) × k_{nAADME}.

(**BCKDH**) enzymes. The reversible transamination of Leu, Ile, and Val is followed by the irreversible oxidative decarboxylation. Transamination of all 3 is catalyzed by BCAA transaminase, and oxidation is catalyzed by BCKDH (Harper et al., 1984). Both enzymes have been detected in bovine mammary glands (Webb et al., 2019), and they are known to play an important role in the mammary glands as demonstrated by an excess of BCAA extraction with the amine group and some of the carbon skeletons contributing to NEAA synthesis (Wohlt et al., 1977; Hanigan et al., 2001; Hanigan et al., 2002). Because the 3 AA share the same catabolic routes, their use is subject to competitive inhibition. However, an excess of any of the BCAA has been shown to stimulate expression of the catabolic enzymes, resulting in increased catabolism of all 3 BCAA. High

dietary Leu in pigs increased BCKDH activity and caused increased oxidation of all 3 BCAA (Wiltafsky et al., 2010; Wessels et al., 2016). However, Ile has been shown to only slightly increase BCKDH activity in rat skeletal muscle, and Val had no effect (Aftring et al., 1986). High concentrations of Val and Ile individually had little effect on increasing catabolism of the other BCAA, especially compared with the effects of high concentrations of Leu in growing chicks (D'Mello and Lewis, 1970). These differences could be due to varying affinities of each BCAA for these enzymes; however, the rate constants for transamination and catabolism herein were almost identical for Ile and Leu, and only slightly less for Val, indicating all 3 BCAA are likely to affect enzyme activity in bovine mammary cells.

However, NEAAG did not affect transamination or irreversible-loss rates (Table 6). One may have anticipated that high concentrations of Ala, Glu, and Gln might inhibit net production of those NEAA from BCAA by increasing the reverse rates. The transamination reaction uses α-ketoglutarate as an N acceptor, and this contributes to synthesis of other NEAA and EAA via subsequent transamination (Holeček, 2018).

In addition, HNEAAG increased the rate constant for Val incorporation into protein ($P = 0.04$) and tended to increase the rate constant for Ile incorporation into protein ($P = 0.09$; Table 6). As stated previously, with HNEAAG, the concentrations of NEAAG increased in the intracellular free AA pool (Table 4). When HNEAAG are already inside the cell, there could be less need for increased catabolism of EAA to form NEAA and, therefore, protein synthesis would be the more likely path. However, Doepel et al. (2009) did not observe a response in milk protein to infusions of NEAA in vivo. They hypothesized that sufficient amounts of NEAA were supplied to meet milk-protein-synthesis needs, even with diets formulated to be low in MP. In contrast, NASEM (2021) found that the aggregate of NEAA had a positive effect on milk-protein synthesis when conducting a meta-analysis. Thus, it is unclear if the effects of HNEAAG observed herein would translate to effects in vivo.

The rate constant for Val incorporation into the fast protein synthesis pool ($k_{nAAtfAA}$) was decreased with HVal, but the constants for Ile and Leu were unchanged (Table 6). This likely represents the mitigation of responses to individual AA via the additive integration of signals arising from multiple AA, energy supply, and hormonal state (Arriola Apelo et al., 2014). The complicated response surface created by those individual factors would not be fully represented by a simple linear function of Val, and thus resulted in the apparent decline in the mass-action constant. This effect may indicate autophagy downregulation with HVal. Amino acids act as nutrient signals to upregulate autophagy genes when deficient (Shen et al., 2021); thus, if supplemented adequately, autophagy would be upregulated. Consistent with the idea of multiple additive control factors, Yoder et al. (2021) observed the greatest fast protein rate constants for most EAA in bovine MEC with the lowest concentration of all AA; however, they did not observe this with NEAA, except for Pro.

Fluxes and Concentrations of Ala, Met, Phe, and Thr

Unfortunately, of the NEAAG we were only able to model Ala. We were unable to differentiate between the U-[^{15}N] and U-[^{13}C] isotopes of Gly on the GCMS because they have the same molecular weight, and Gln is undetectable in both U-[^{15}N]- and U-[^{13}C]-AA prepared from algal protein due to destruction during the hydrolysis process. Although we supplemented the [^{13}C]-labeled media with additional [^{13}C]-Gln, we failed to supplement the [^{15}N]-labeled media, which compromised model fits for that AA (Supplemental Table S2).

Net uptake of Ala was negative with the LNEAAG treatment (Table 3). This reflects an approximate halving of the influx (F_{xAAnAA}), efflux (F_{nAAxAA}), and transamination (F_{nAAnKA}) rates, as well as numerical reductions in synthesis rates ($F_{Synthesis}$), which resulted in a slight imbalance and net export of Ala. Alanine can be formed by transamination using the amine group from the BCAA, and net uptake was most negative in the HVal and LNEAAG treatment, indicating increased synthesis from Val.

Net uptake, influx, and incorporation of Ala into fast protein fluxes significantly increased with HNEAAG ($P < 0.01$, $P = 0.02$, and $P = 0.04$, respectively; Table 3). In addition, the deamination and reamination fluxes for Ala both tended to increase with HNEAAG treatment ($P = 0.06$). These effects are largely driven by mass action, because Ala was part of the NEAAG treatment. Furthermore, intracellular Ala concentrations increased (Table 4), a result that supports transamination changes. It is unclear if the increased incorporation of Ala into fast protein was driven directly by increased Ala concentrations or indirectly by increased EAA concentrations, but the latter seems more likely given current knowledge.

The EAA Met, Phe, and Thr were of interest because they share the System L transporters with the BCAA. However, Phe is thought to be primarily transported by LAT1 transporters with greater affinity than the BCAA (Kanai et al., 1998) and is only transported by transporters shared with the BCAA (Bröer and Bröer, 2017). In contrast, Met and Thr are also transported by System A and System ASC transporters (Bröer and Bröer, 2017), respectively, but Ile and Leu are not, and

Val is transported with very low affinity by System ASC.

The efflux of Met increased with HNEAAG ($P = 0.01$; Table 3). This was not driven by intracellular Met concentrations, which were reduced with HNEAG. Thus it must reflect the exchange-substrate effects of greater extracellular concentrations of NEAAG. It is unclear why the extracellular NEAAG substrate effects would dominate the intracellular effects, but it clearly indicates a transporter activity change, rather than mass-action effects. Met has many routes for entering the cell, including both exchange and Na-dependent transporters (Bröer and Bröer, 2017), which may explain the lack of Val effects on Met.

Interestingly, a significant treatment interaction occurred for the Met irreversible-loss flux ($F_{DMEAAIL}$). This effect was driven by the very high irreversible-loss flux for the LVal, LNEAAG treatment compared to the HVal, LNEAAG treatment. When Met is irreversibly lost, it forms NEAA including Gly and Cys (Finkelstein, 1990). It appears that when Val is low in concert with low NEAAG, Met is likely in excess of cellular needs, leading to enhanced irreversible loss.

Net uptake of Phe was negative for all treatments, and not significantly affected by treatment (Table 3). This was also observed by Yoder et al. (2021). Phenylalanine is present in very high concentrations in algae, leading to much higher IR for Phe than for the other AA. The very low unlabeled concentrations of Phe in both [^{15}N]- and [^{13}C]-labeled treatment media caused higher variance compared with other AA, which was propagated in model simulations. The IR was approximately 16.8 for Phe in the [^{13}C]-labeled media; thus, if the unlabeled media concentrations decreased from 9 μM to just 7 μM, the total concentration would decrease by approximately 22%. If real, negative net uptake may reflect possible protein degradation, meaning that Phe could have been deficient in the system, but this was not apparent from net balances of the other AA.

Influx of Phe significantly increased with the HNEAAG treatment ($P < 0.01$), but efflux was not affected. Furthermore, intracellular free concentrations of Phe decreased with HNEAAG (Table 4), which is consistent with negative balance. There were significant interactions for the transamination and irreversible-loss fluxes ($P < 0.01$ and $P = 0.03$, respectively), but these fluxes were much too small to explain the negative net uptake. The comparatively low transamination fluxes are not in agreement with Hanigan et al. (2009), where high transamination rates of Phe were found in the mammary glands. In the same paper, it was deduced that Phe metabolism results in a substantial loss of the ^{15}N label but little loss of the C labels. Because deamination does not occur before oxidation to Tyr, perhaps a label-return problem exists within the current model. Subsequent work should include the Tyr observations so a direct estimate of Phe-to-Tyr flux can be estimated. It is possible that the more complicated kinetics of Phe resulted in deamination and reamination calculations biasing the uptake measurements, as noted by the difference in relative amination rates as compared with Hanigan et al. (2009).

The rate of protein synthesis decreased with the HNEAAG treatment ($P < 0.01$) and also in response to HVal ($P = 0.05$). However, protein-bound concentrations of Phe were unaffected by treatment, and therefore there were no indications that the cells were catabolizing net amounts of cell protein to support the net export of Phe.

The HNEAAG treatment significantly decreased rates of Thr transamination and irreversible loss ($P = 0.02$ and $P = 0.03$, respectively), and the remaining fluxes were unaffected by treatment (Table 3). However, the mean intracellular free concentrations of Thr decreased with HNEAAG (Table 4), which is inconsistent with the apparent decline in use. A numerical increase in influx occurred with HNEAAG; if real, this may explain the increase in intracellular Thr concentrations.

Rate Constants for Ala, Met, Phe, and Thr

The rate constant estimates for Ala synthesis, efflux, tissue-protein synthesis, and transamination were unaffected by treatment, indicating the flux changes were driven by mass action (Table 6). However, HNEAAG, which included Ala, decreased the constant for uptake ($P < 0.001$), which could reflect a reduction in transporter expression or that the response moved into the mixed-order range of a nonlinear response surface. A decline in transporter activity is consistent with the previous observations of reduced SNAT2 transporter expression with Ala supplementation (López et al., 2006).

The rate constants for Met influx, protein synthesis, and catabolism were not affected by treatment, but the efflux rate constant decreased with HNEAAG ($P = 0.05$; Table 6), which was consistent with the change in efflux rates and numerical declines in intracellular concentrations (Table 4). Because Met shares System A transport with the NEAA contained in the NEAAG treatment (Bröer and Bröer, 2017), it is possible that the elevated intracellular concentrations of the NEAAG with the HNEAAG treatment competitively inhibited efflux (Table 3), which would be reflected in the rate constant (Table 6). However, Met is transported more by System L transporters compared to System A transporters (Shotwell et al., 1981); in addition, Met is a good efflux substrate for the System

L transporters, but a relatively poor influx substrate (Verrey, 2003). Thus, it is more likely that the efflux affinity was downregulated for the System L transporters with the increase of intracellular concentrations of the NEAAG.

The influx rate constant for Phe significantly increased with HNEAAG treatment ($P = 0.02$; Table 6). As with the BCAA, Phe is transported by System L transporters (Bröer and Bröer, 2017). The increased influx constant with HNEAAG suggests that Phe transport by the exchange transporters represents a significant proportion of the total transport in bovine MEC. The rate constant for protein synthesis was also decreased by HNEAAG ($P = 0.03$). Rate constants for transamination were extremely low, resulting in a significant treatment effect for NEAAG, Val, and a significant interaction. If real, the HVal combined with HNEAAG treatment resulted in the greatest transamination activity for Phe. However, it is important to note that the transamination activities observed herein were much lower in comparison to tissue-protein synthesis than that observed in vivo by Hanigan et al. (2009). Perhaps the closed in vitro system limits the transamination activity of Phe.

The influx rate constant for Thr did not change with treatment, but the efflux rate constant tended to increase ($P = 0.07$) with an interaction of HNEAAG and LVal (Table 6). This is very similar to the effects seen in Ile and Leu. Furthermore, there was a significant interaction for the fast-protein-synthesis rate constant ($P = 0.04$) and a tendency for an interaction of the transamination rate constant ($P = 0.09$).

General Implications

The use of the primary MEC model is a less costly and more controlled way to study the epithelial cell function of bovine mammary glands. The cells were making protein in general as indicated by cell growth and by incorporation of isotopes into cell protein. Furthermore, casein production by these MEC was observed in a prior experiment (Ruiz-Cortés et al., 2022). Thus they appear representative, but findings must be verified in vivo.

Uptake of AA into MEC was generally about double net uptake, which offers metabolic flexibility to allow changes in efflux to complement or compensate for changes in influx, and the changes in transport activity driven by the supply of the NEAA and Val underscore the intricacies of metabolic regulation in the tissue.

The apparent competitive inhibition of Val on uptake of Leu and Ile is consistent with the negative effects of absorbed Val on milk-protein production reported by NASEM (2021). This combination of observations suggests that dairy diets may generally provide an excess of Val relative to minimum needs. Clearly, Val is a required AA, and if one assumes the underlying basic response is similar to Ile or Leu, a tradeoff may exist between the positive effects of Val as a regulator of protein synthesis and the negative effects of competitive inhibition of Ile and Leu transport. If Val is much less potent in stimulating protein synthesis than Ile and Leu, the response surface may be negative until mass balance limits Val availability as a substrate.

Valine is considered the fourth "limiting amino acid" in broiler chickens fed a typical corn–soy diet (Corzo et al., 2009), and has been shown to enhance growth of broilers when supplemented into a low-CP diet (Ospina-Rojas et al., 2014). Because a lot of corn- and soybean-based protein is also fed to dairy cattle, one might expect positive responses with cattle as well, which makes the negative effects interesting in this case. However, Val may reach a benefit threshold before causing negative effects. Haque et al. (2013) observed a 4.9% decrease in milk-protein content with a Val-deficient diet in lactating dairy cows. However, there does not appear to be work examining protein-production responses to infusion of Val into dairy cows to test this hypothesis.

The effects of NEAA on transport of several System L AA have major potential implications. The general goal with protein feeding across production species has been to reduce CP and supplement with selected EAA to match an estimated ideal profile. The reduction in CP with no addition of NEAA may be compromising the intent with respect to lactational performance. Leucine, Ile, and Met are all relatively effective in stimulating mechanistic target of rapamycin (mTOR) activity (Appuhamy et al., 2012), are all transported by System L, and thus all 3 may be susceptible to the effects of low concentrations of NEAA. Based on the relatively small, but highly significant, positive slope coefficient for NEAA in the NASEM (2021) milk-protein equation, the relatively large changes in influx observed herein must be partially mitigated, but not negated, by other regulatory elements. Glycine, a required AA for poultry, is commonly supplemented in those systems (Ospina-Rojas et al., 2014). Furthermore, supplemented Gly in low-protein diets (low-protein diet = 12.03% CP vs. normal = 16% CP) for swine has been shown to improve growth performance and meat quality (Jiang et al., 2023). Because of its large-scale production, Gly is relatively inexpensive, and thus if N excretion is monetized, feeding rumen-protected Gly plus other EAA within a low-CP diet may be economically and environmentally favorable. Although from this data

alone it is impossible to identify the individual effects of Gly, NEAAG was shown to stimulate transport activity of multiple EAA.

Interestingly, the uptake of Gly increased when EAA were infused (Doepel et al., 2009), which could reflect increased requirements of NEAA under high-EAA conditions. However, it is important to note that sometimes, when supplementing NEAA, the uptake of Gly can become negative (Doepel et al., 2009), indicating that Gly synthesis in the mammary glands also plays a significant role. Because of the roles of Arg in increasing de novo fatty acid synthesis in dairy cows (Ding et al., 2022) and for a variety of benefits in monogastrics such as activating proliferative mechanisms in the mammary glands of lactating sows (Holanda et al., 2019), it is currently being studied as a supplement. Arginine is also taken up in excess by the mammary glands, due to its role as a precursor for ornithine; ornithine has been shown to be a precursor for Ala, Asp, Glu, Ser, and Gly in perfused mammary glands (Roets et al., 1979). However, Doepel and Lapierre (2011) observed no change in milk-protein yield with the deletion of Arg from a low-protein diet; but more work is needed to elucidate the potential effects of supplemented Arg as a precursor for NEAA, which could aid in EAA transport and increased AA efficiency.

Future Directions

The new milk-protein model in the NASEM (2021) model should stimulate development and supply of additional rumen-protected AA other than Lys and Met. Moving forward, it will be important to characterize the full response surface for all of the EAA and consider possible synergisms and antagonisms among AA, including the NEAA.

CONCLUSIONS

Valine influx, efflux, transamination, and irreversible loss, but not tissue-protein synthesis, appear to be mostly driven by mass action. However, Val rate constants for incorporation into rapidly exchanging tissue protein, transamination, and irreversible loss decreased with HVal, which could indicate downregulation of activity or saturation of those processes. The latter appears to be the case because the rate constants for transamination and irreversible loss of Ile and Leu were also downregulated with HVal. This result could be attributed to competition for shared transamination and oxidation enzymes or a reduction in enzymatic activity. The importance of NEAA is evidenced by apparent stimulation of the influx and efflux rate constants for both Val and Leu with HNEAAG. Interestingly, antagonization of the influx and efflux rate constants of Val on Ile and Leu was only observed when coupled with HNEAAG, indicating important interactive effects for AA transport. As a whole, these results provide evidence for complicated AA antagonisms and synergisms that may affect in vivo animal performance.

ACKNOWLEDGMENTS

The authors appreciate the labor of G. Kawecki and other students within the Hanigan Laboratory (School of Animal Sciences, Virginia Tech, Blacksburg, VA). The work was funded in part by the Virginia Agricultural Experiment Station and the Hatch Program of the National Institute of Food and Agriculture (NIFA), USDA via the NC-2040 regional research project, the Virginia Tech College of Agriculture and Life Sciences David R. and Margaret Lincicome Endowment (Blacksburg, VA), Balchem Corp (Montvale, NJ), and USDA-NIFA (Kansas City, MO; Grant #2021-07170). General departmental support was provided by the Virginia State Dairymen's Association (Bridgewater, VA). A. Hruby Weston conducted sample collection, sample analysis, modeling analyses, and statistical analyses, and drafted the manuscript with the assistance of M. D. Hanigan. P. S. Yoder designed the experiment, I. A. M. A. Teixeira provided data collection support, and T. Pilonero was the technical specialist for laboratory analysis. All authors participated in manuscript edits. The authors have not stated any conflicts of interest.

REFERENCES

Aftring, R. P., K. P. Block, and M. G. Buse. 1986. Leucine and isoleucine activate skeletal muscle branched-chain alpha-keto acid dehydrogenase in vivo. Am. J. Physiol. Endocrinol. Metab. 250:E599–E604. https://doi.org/10.1152/ajpendo.1986.250.5.E599.

Appuhamy, J. A., N. A. Knoebel, W. A. Nayananjalie, J. Escobar, and M. D. Hanigan. 2012. Isoleucine and leucine independently regulate mTOR signaling and protein synthesis in MAC-T cells and bovine mammary tissue slices. J. Nutr. 142:484–491. https://doi.org/10.3945/jn.111.152595.

Appuhamy, J. A. D. R. N., W. A. Nayananjalie, E. M. England, D. E. Gerrard, R. M. Akers, and M. D. Hanigan. 2014. Effects of AMP-activated protein kinase (AMPK) signaling and essential amino acids on mammalian target of rapamycin (mTOR) signaling and protein synthesis rates in mammary cells. J. Dairy Sci. 97:419–429. https://doi.org/10.3168/jds.2013-7189.

Arriola Apelo, S. I., J. R. Knapp, and M. D. Hanigan. 2014. Invited review: Current representation and future trends of predicting amino acid utilization in the lactating dairy cow. J. Dairy Sci. 97:4000–4017. https://doi.org/10.3168/jds.2013-7392.

Arriza, J. L., M. P. Kavanaugh, W. A. Fairman, Y. N. Wu, G. H. Murdoch, R. A. North, and S. G. Amara. 1993. Cloning and expression of a human neutral amino acid transporter with structural similarity to the glutamate transporter gene family. J. Biol. Chem. 268:15329–15332. https://doi.org/10.1016/S0021-9258(18)82257-8.

Baik, M., B. Etchebarne, J. Bong, and M. VandeHaar. 2009. Gene expression profiling of liver and mammary tissues of lactating dairy cows. Asian-Australas. J. Anim. Sci. 22:871–884. https://doi.org/10.5713/ajas.2009.90061.

Baumrucker, C. R. 1984. Cationic amino acid transport by bovine mammary tissue. J. Dairy Sci. 67:2500–2506. https://doi.org/10.3168/jds.S0022-0302(84)81606-9.

Bibby, J., and H. Toutenburg. 1977. Prediction and Improved Estimation in Linear Models. Wiley.

Bröer, S. 2008. Amino acid transport across mammalian intestinal and renal epithelia. Physiol. Rev. 88:249–286. https://doi.org/10.1152/physrev.00018.2006.

Bröer, S., and A. Bröer. 2017. Amino acid homeostasis and signalling in mammalian cells and organisms. Biochem. J. 474:1935–1963. https://doi.org/10.1042/BCJ20160822.

Calder, A. G., K. E. Garden, S. E. Anderson, and G. E. Lobley. 1999. Quantitation of blood and plasma amino acids using isotope dilution electron impact gas chromatography/mass spectrometry with U-(13)C amino acids as internal standards. Rapid Commun. Mass Spectrom. 13:2080–2083. https://doi.org/10.1002/(SICI)1097-0231(19991115)13:21<2080::AID-RCM755>3.0.CO;2-O.

Chen, F., S. Zhang, Z. Deng, Q. Zhou, L. Cheng, S. W. Kim, J. Chen, and W. Guan. 2018. Regulation of amino acid transporters in the mammary gland from late pregnancy to peak lactation in the sow. J. Anim. Sci. Biotechnol. 9:35. https://doi.org/10.1186/s40104-018-0250-4.

Chillarón, J., R. Estévez, C. Mora, C. A. Wagner, H. Suessbrich, F. Lang, J. L. Gelpí, X. Testar, A. E. Busch, A. Zorzano, and M. Palacín. 1996. Obligatory amino acid exchange via systems bo,+-like and y+L-like. A tertiary active transport mechanism for renal reabsorption of cystine and dibasic amino acids. J. Biol. Chem. 271:17761–17770. https://doi.org/10.1074/jbc.271.30.17761.

Christensen, H. N. 1990. Role of amino acid transport and countertransport in nutrition and metabolism. Physiol. Rev. 70:43–77. https://doi.org/10.1152/physrev.1990.70.1.43.

Corzo, A., R. Loar II, and M. Kidd. 2009. Limitations of dietary isoleucine and valine in broiler chick diets. Poult. Sci. 88:1934–1938. https://doi.org/10.3382/ps.2009-00109.

D'Mello, J. P., and D. Lewis. 1970. Amino acid interactions in chick nutrition. 2. Interrelationships between leucine, isoleucine and valine. Br. Poult. Sci. 11:313–323. https://doi.org/10.1080/00071667008415821.

Ding, L., Y. Shen, M. Jawad, T. Wu, S. K. Maloney, M. Wang, N. Chen, and D. Blache. 2022. Effect of arginine supplementation on the production of milk fat in dairy cows. J. Dairy Sci. 105:8115–8129. https://doi.org/10.3168/jds.2021-21312.

Doelman, J., J. J. M. Kim, M. Carson, J. A. Metcalf, and J. P. Cant. 2015. Branched-chain amino acid and lysine deficiencies exert different effects on mammary translational regulation. J. Dairy Sci. 98:7846–7855. https://doi.org/10.3168/jds.2015-9819.

Doepel, L., and H. Lapierre. 2011. Deletion of arginine from an abomasal infusion of amino acids does not decrease milk protein yield in Holstein cows. J. Dairy Sci. 94:864–873. https://doi.org/10.3168/jds.2010-3497.

Doepel, L., G. E. Lobley, J. F. Bernier, P. Dubreuil, and H. Lapierre. 2009. Differences in splanchnic metabolism between late gestation and early lactation dairy cows. J. Dairy Sci. 92:3233–3243. https://doi.org/10.3168/jds.2008-1595.

Finkelstein, J. D. 1990. Methionine metabolism in mammals. J. Nutr. Biochem. 1:228–237. https://doi.org/10.1016/0955-2863(90)90070-2.

Forde, N., C. A. Simintiras, R. Sturmey, S. Mamo, A. K. Kelly, T. E. Spencer, F. W. Bazer, and P. Lonergan. 2014. Amino acids in the uterine luminal fluid reflects the temporal changes in transporter expression in the endometrium and conceptus during early pregnancy in cattle. PLoS One 9:e100010. https://doi.org/10.1371/journal.pone.0100010.

França, M. R., M. I. S. da Silva, G. Pugliesi, V. Van Hoeck, and M. Binelli. 2017. Evidence of endometrial amino acid metabolism and transport modulation by peri-ovulatory endocrine profiles driving uterine receptivity. J. Anim. Sci. Biotechnol. 8:54. https://doi.org/10.1186/s40104-017-0185-1.

Fu, L., L. Zhang, L. Liu, H. Yang, P. Zhou, F. Song, G. Dong, J. Chen, G. Wang, and X. Dong. 2021. Effect of heat stress on bovine mammary cellular metabolites and gene transcription related to amino acid metabolism, amino acid transportation and mammalian target of rapamycin (mTOR) signaling. Animals (Basel) 11:3153. https://doi.org/10.3390/ani11113153.

Hanigan, M., H. Bateman, J. Fadel, and J. McNamara. 2006. Metabolic models of ruminant metabolism: recent improvements and current status. J. Dairy Sci. 89:E52–E64. https://doi.org/10.3168/jds.S0022-0302(06)72363-3.

Hanigan, M., L. Crompton, B. Bequette, J. Mills, and J. France. 2002. Modelling mammary metabolism in the dairy cow to predict milk constituent yield, with emphasis on amino acid metabolism and milk protein production: Model evaluation. J. Theor. Biol. 217:311–330. https://doi.org/10.1006/jtbi.2002.3037.

Hanigan, M., L. Crompton, J. Metcalf, and J. France. 2001. Modelling mammary metabolism in the dairy cow to predict milk constituent yield, with emphasis on amino acid metabolism and milk protein production: Model construction. J. Theor. Biol. 213:223–239. https://doi.org/10.1006/jtbi.2001.2417.

Hanigan, M. D., J. France, L. A. Crompton, and B. J. Bequette. 2000. Evaluation of a Representation of the Limiting Amino Acid Theory for Milk Protein Synthesis. Pages 127–144. CABI, Wallingford.

Hanigan, M. D., J. France, S. J. Mabjeesh, W. C. McNabb, and B. J. Bequette. 2009. High rates of mammary tissue protein turnover in lactating goats are energetically costly. J. Nutr. 139:1118–1127. https://doi.org/10.3945/jn.108.103002.

Haque, M. N., H. Rulquin, and S. Lemosquet. 2013. Milk protein responses in dairy cows to changes in postruminal supplies of arginine, isoleucine, and valine. J. Dairy Sci. 96:420–430. https://doi.org/10.3168/jds.2012-5610.

Harper, A. E., R. H. Miller, and K. P. Block. 1984. Branched-chain amino acid metabolism. Annu. Rev. Nutr. 4:409–454. https://doi.org/10.1146/annurev.nu.04.070184.002205.

Harris, R. A., M. Joshi, N. H. Jeoung, and M. Obayashi. 2005. Overview of the molecular and biochemical basis of branched-chain amino acid catabolism. J. Nutr. 135:1527S–1530S. https://doi.org/10.1093/jn/135.6.1527S.

Holanda, D. M., C. S. Marcolla, S. E. F. Guimarães, M. M. Neves, G. J. Hausman, M. S. Duarte, M. L. T. Abreu, and A. Saraiva. 2019. Dietary L-arginine supplementation increased mammary gland vascularity of lactating sows. Animal 13:790–798. https://doi.org/10.1017/S1751731118002069.

Holeček, M. 2018. Branched-chain amino acids in health and disease: metabolism, alterations in blood plasma, and as supplements. Nutr. Metab. (Lond.) 15:33. https://doi.org/10.1186/s12986-018-0271-1.

Horn, F., and R. Jackson. 1972. General mass action kinetics. Arch. Ration. Mech. Anal. 47:81–116. https://doi.org/10.1007/BF00251225.

Hruby, A., I. A. M. A. Teixeira, P. S. Yoder, T. Pilonero, and M. D. Hanigan. 2023. Valine and non-essential amino acids affect bi-directional transport rates of leucine and isoleucine in bovine mammary epithelial cells. University Libraries, Virginia Tech. Dataset. https://doi.org/10.7294/24042825.v2.

Hu, H., J. Wang, D. Bu, H. Wei, L. Zhou, F. Li, and J. J. Loor. 2009. In vitro culture and characterization of a mammary epithelial cell line from Chinese Holstein dairy cow. PLoS One 4:e7636. https://doi.org/10.1371/journal.pone.0007636.

Jackson, S. C., J. M. Bryson, H. Wang, and W. L. Hurley. 2000. Cellular uptake of valine by lactating porcine mammary tissue. J. Anim. Sci. 78:2927–2932. https://doi.org/10.2527/2000.78112927x.

Jiang, S., W. Quan, J. Luo, A. Lou, X. Zhou, F. Li, and Q. W. Shen. 2023. Low-protein diets supplemented with glycine improves pig growth performance and meat quality: An untargeted metabolomic analysis. Front. Vet. Sci. 10:1170573. https://doi.org/10.3389/fvets.2023.1170573.

Kanai, Y., H. Segawa, K.-i. Miyamoto, H. Uchino, E. Takeda, and H. Endou. 1998. Expression cloning and characterization of a transporter for large neutral amino acids activated by the heavy chain of 4F2 antigen (CD98). J. Biol. Chem. 273:23629–23632. https://doi.org/10.1074/jbc.273.37.23629.

Krishnamurthy, R. V., Y. R. Suryawanshi, and K. Essani. 2017. Nitrogen isotopes provide clues to amino acid metabolism in human colorectal cancer cells. Sci. Rep. 7:2562. https://doi.org/10.1038/s41598-017-02793-y.

Lee, C., A. N. Hristov, T. W. Cassidy, K. S. Heyler, H. Lapierre, G. A. Varga, M. J. de Veth, R. A. Patton, and C. Parys. 2012. Rumen-protected lysine, methionine, and histidine increase milk protein yield in dairy cows fed a metabolizable protein-deficient diet. J. Dairy Sci. 95:6042–6056. https://doi.org/10.3168/jds.2012-5581.

Li, P., D. A. Knabe, S. W. Kim, C. J. Lynch, S. M. Hutson, and G. Wu. 2009. Lactating porcine mammary tissue catabolizes branched-chain amino acids for glutamine and aspartate synthesis. J. Nutr. 139:1502–1509. https://doi.org/10.3945/jn.109.105957.

Lin, L. I.-K. 1989. A concordance correlation coefficient to evaluate reproducibility. Biometrics 45:255–268. https://doi.org/10.2307/2532051. PubMed

Lin, Y., X. Duan, H. Lv, Y. Yang, Y. Liu, X. Gao, and X. Hou. 2018. The effects of L-type amino acid transporter 1 on milk protein synthesis in mammary glands of dairy cows. J. Dairy Sci. 101:1687–1696. https://doi.org/10.3168/jds.2017-13201.

López, A., N. Torres, V. Ortiz, G. Alemán, R. Hernández-Pando, and A. R. Tovar. 2006. Characterization and regulation of the gene expression of amino acid transport system A (SNAT2) in rat mammary gland. Am. J. Physiol. Endocrinol. Metab. 291:E1059–E1066. https://doi.org/10.1152/ajpendo.00062.2006.

Maas, J. A., J. France, J. Dijkstra, A. Bannink, and B. W. McBride. 1998. Application of a mechanistic model to study competitive inhibition of amino acid uptake by the lactating bovine mammary gland. J. Dairy Sci. 81:1724–1734. https://doi.org/10.3168/jds.S0022-0302(98)75740-6.

Martineau, R., D. R. Ouellet, E. Kebreab, R. R. White, and H. Lapierre. 2017. Relationships between postruminal casein infusion and milk production, and concentrations of plasma amino acids and blood urea in dairy cows: A multilevel mixed-effects meta-analysis. J. Dairy Sci. 100:8053–8071. https://doi.org/10.3168/jds.2016-11813.

NASEM (National Academy of Science, Engineering, and Medicine). 2021. Nutrient Requirements of Dairy Cattle. 8th rev. ed. The National Academies Press, Washington, DC.

NRC. 2001. Nutrient Requirements of Dairy Cattle. 7th rev. ed. The National Academies Press, Washington, DC.

Ospina-Rojas, I., A. Murakami, C. Duarte, C. Eyng, C. Oliveira, and V. Janeiro. 2014. Valine, isoleucine, arginine and glycine supplementation of low-protein diets for broiler chickens during the starter and grower phases. Br. Poult. Sci. 55:766–773. https://doi.org/10.1080/00071668.2014.970125.

Oxender, D. L., and H. N. Christensen. 1963. Distinct mediating systems for the transport of neutral amino acids by the Ehrlich cell. J. Biol. Chem. 238:3686–3699. https://doi.org/10.1016/S0021-9258(19)75327-7.

Patton, R. A. 2010. Effect of rumen-protected methionine on feed intake, milk production, true milk protein concentration, and true milk protein yield, and the factors that influence these effects: A meta-analysis. J. Dairy Sci. 93:2105–2118. https://doi.org/10.3168/jds.2009-2693.

Pfeiffer, R., G. Rossier, B. Spindler, C. Meier, L. Kühn, and F. Verrey. 1999. Amino acid transport of y+ L-type by heterodimers of 4F2hc/CD98 and members of the glycoprotein-associated amino acid transporter family. EMBO J. 18:49–57. https://doi.org/10.1093/emboj/18.1.49.

R Core Team. 2022. R: A Language and Environment for Statistical Computing. R Foundation for Statistical Computing, Vienna, Austria.

Roets, E., R. Verbeke, G. Peeters, H. Axmann, and G. Proksch. 1979. Metabolism of ornithine in perfused goat udder. J. Dairy Sci. 62:259–269. https://doi.org/10.3168/jds.S0022-0302(79)83234-8.

Ruiz-Cortés, Z. T., P. Yoder, and M. D. Hanigan. 2022. Effects of essential amino acid deficiency on general control nonderepressible 2/eukaryotic initiation factor 2 signaling and proteomic changes in primary bovine mammary epithelial cells. Curr. Issues Mol. Biol. 44:1075–1086. https://doi.org/10.3390/cimb44030071.

Rulquin, H., and L. Delaby. 1997. Effects of the energy balance of dairy cows on lactational responses to rumen-protected methionine. J. Dairy Sci. 80:2513–2522. https://doi.org/10.3168/jds.S0022-0302(97)76204-0.

Rulquin, H., and P. M. Pisulewski. 2006. Effects of graded levels of duodenal infusions of leucine on mammary uptake and output in lactating dairy cows. J. Dairy Res. 73:328–339. https://doi.org/10.1017/S0022029906001841.

Schwab, C. G., L. D. Satter, and A. B. Clay. 1976. Response of lactating dairy cows to abomasal infusion of amino acids. J. Dairy Sci. 59:1254–1270. https://doi.org/10.3168/jds.S0022-0302(76)84354-8.

Seymour, W. M., C. E. Polan, and J. H. Herbein. 1990. Effects of dietary protein degradability and casein or amino acid infusions on production and plasma amino acids in dairy cows. J. Dairy Sci. 73:735–748. https://doi.org/10.3168/jds.S0022-0302(90)78727-9.

Shen, J. Z., G. Wu, and S. Guo. 2021. Amino acids in autophagy: Regulation and function. Adv. Exp. Med. Biol. 1332:51–66. https://doi.org/10.1007/978-3-030-74180-8_4.

Shennan, D. B., and C. A. Boyd. 2014. The functional and molecular entities underlying amino acid and peptide transport by the mammary gland under different physiological and pathological conditions. J. Mammary Gland Biol. Neoplasia 19:19–33. https://doi.org/10.1007/s10911-013-9305-5.

Shotwell, M. A., D. Jayme, M. Kilberg, and D. Oxender. 1981. Neutral amino acid transport systems in Chinese hamster ovary cells. J. Biol. Chem. 256:5422–5427. https://doi.org/10.1016/S0021-9258(19)69218-5.

Soetaert, K., and T. Petzoldt. 2010. Inverse modelling, sensitivity and Monte Carlo analysis in R using package FME. J. Stat. Softw. 33. https://doi.org/10.18637/jss.v033.i03.

Soetaert, K., T. Petzoldt, and R. W. Setzer. 2010. Solving differential equations in R: package deSolve. J. Stat. Softw. 33:1–25. https://doi.org/10.18637/jss.v033.i09.

Sperringer, J. E., A. Addington, and S. M. Hutson. 2017. Branched-chain amino acids and brain metabolism. Neurochem. Res. 42:1697–1709. https://doi.org/10.1007/s11064-017-2261-5.

Taylor, P. M. 2014. Role of amino acid transporters in amino acid sensing. Am. J. Clin. Nutr. 99:223S–230S. https://doi.org/10.3945/ajcn.113.070086.

Tian, W., H. R. Wang, T. Y. Wu, L. Y. Ding, R. Zhao, E. Khas, C. F. Wang, F. Q. Zhang, F. Y. Mi, L. Wang, and L. T. Ning. 2017. Milk protein responses to balanced amino acid and removal of leucine and arginine supplied from jugular-infused amino acid mixture in lactating dairy cows. J. Anim. Physiol. Anim. Nutr. (Berl.) 101:e278–e287. https://doi.org/10.1111/jpn.12603.

Torres, N., A. R. Tovar, and A. E. Harper. 1995. Leucine affects the metabolism of valine by isolated perfused rat hearts: Relation to branched-chain amino acid antagonism. J. Nutr. 125:1884–1893. https://doi.org/10.1093/jn/125.7.1884.

Vanhatalo, A., P. Huhtanen, V. Toivonen, and T. Varvikko. 1999. Response of dairy cows fed grass silage diets to abomasal infusions of histidine alone or in combinations with methionine and lysine. J. Dairy Sci. 82:2674–2685. https://doi.org/10.3168/jds.S0022-0302(99)75524-4.

Verrey, F. 2003. System L: Heteromeric exchangers of large, neutral amino acids involved in directional transport. Pflugers Arch. 445:529–533. https://doi.org/10.1007/s00424-002-0973-z.

Villanueva, R. A. M., and Z. J. Chen. 2019. ggplot2: Elegant Graphics for Data Analysis 2nd ed. Measurement (Mahwah, NJ) 17:160–167. https://doi.org/10.1080/15366367.2019.1565254.

Walsh, R. G., S. He, and C. T. Yarnes. 2014. Compound-specific δ13C and δ15N analysis of amino acids: A rapid, chloroformate-based method for ecological studies. Rapid Commun. Mass Spectrom. 28:96–108. https://doi.org/10.1002/rcm.6761.

Webb, L. A., H. Sadri, D. von Soosten, S. Dänicke, S. Egert, P. Stehle, and H. Sauerwein. 2019. Changes in tissue abundance and activity of enzymes related to branched-chain amino acid catabolism in dairy cows during early lactation. J. Dairy Sci. 102:3556–3568. https://doi.org/10.3168/jds.2018-14463.

Wessels, A. G., H. Kluge, F. Hirche, A. Kiowski, A. Schutkowski, E. Corrent, J. Bartelt, B. König, and G. I. Stangl. 2016. High leucine

diets stimulate cerebral branched-chain amino acid degradation and modify serotonin and ketone body concentrations in a pig model. PLoS One 11:e0150376. https://doi.org/10.1371/journal.pone.0150376.

Wiltafsky, M. K., M. W. Pfaffl, and F. X. Roth. 2010. The effects of branched-chain amino acid interactions on growth performance, blood metabolites, enzyme kinetics and transcriptomics in weaned pigs. Br. J. Nutr. 103:964–976. https://doi.org/10.1017/S0007114509992212.

Wohlt, J. E., J. H. Clark, R. G. Derrig, and C. L. Davis. 1977. Valine, leucine, and isoleucine metabolism by lactating bovine mammary tissue. J. Dairy Sci. 60:1875–1882. https://doi.org/10.3168/jds.S0022-0302(77)84118-0.

Wu, G. 2013. Functional amino acids in nutrition and health. Amino Acids 45:407–411. https://doi.org/10.1007/s00726-013-1500-6.

Yanagida, O., Y. Kanai, A. Chairoungdua, D. K. Kim, H. Segawa, T. Nii, S. H. Cha, H. Matsuo, J.-i. Fukushima, Y. Fukasawa, Y. Tani, Y. Taketani, H. Uchino, J. Y. Kim, J. Inatomi, I. Okayasu, K.-i. Miyamoto, E. Takeda, T. Goya, and H. Endou. 2001. Human L-type amino acid transporter 1 (LAT1): Characterization of function and expression in tumor cell lines. Biochim. Biophys. Acta. 1514:291–302. https://doi.org/10.1016/S0005-2736(01)00384-4.

Yoder, P. S., J. J. Castro, T. Ruiz-Cortes, and M. D. Hanigan. 2020a. An in vitro method for assessment of amino acid bidirectional transport and intracellular metabolic fluxes in mammary epithelial cells. J. Dairy Sci. 103:8948–8966. https://doi.org/10.3168/jds.2020-18155.

Yoder, P. S., J. J. Castro, T. Ruiz-Cortés, and M. D. Hanigan. 2021. Effects of varying extracellular amino acid concentrations on bidirectional amino acid transport and intracellular fluxes in mammary epithelial cells. J. Dairy Sci. 104:9931–9947. https://doi.org/10.3168/jds.2021-20187.

Yoder, P. S., X. Huang, I. A. Teixeira, J. P. Cant, and M. D. Hanigan. 2020b. Effects of jugular infused methionine, lysine, and histidine as a group or leucine and isoleucine as a group on production and metabolism in lactating dairy cows. J. Dairy Sci. 103:2387–2404. https://doi.org/10.3168/jds.2019-17082.

Yoder, P. S., T. Ruiz-Cortes, J. J. Castro, and M. D. Hanigan. 2019. Effects of varying extracellular amino acid profile on intracellular free amino acid concentrations and cell signaling in primary mammary epithelial cells. J. Dairy Sci. 102:8977–8985. https://doi.org/10.3168/jds.2018-16122.

ORCIDS

A. Hruby Weston https://orcid.org/0000-0002-5717-615X
I. A. M. A. Teixeira https://orcid.org/0000-0002-7432-867X
P. S. Yoder https://orcid.org/0000-0001-6646-1991
T. Pilonero https://orcid.org/0000-0001-8666-1712
M. D. Hanigan https://orcid.org/0000-0002-5639-9677